H. T. Hall

OFFICE OF NAVAL RESEARCH

FINAL REPORT

CONTRACT N5ori-07644

TASK NO. NR-032400

Apparatus and Chemistry

PROPERTIES OF MATERIALS AT HIGH PRESSURES AND TEMPERATURES

FRANCIS BIRCH AND EUGENE C. ROBERTSON

DUNBAR LABORATORY

HARVARD UNIVERSITY

MARCH, 1957

Technical Report

Contract N5ori-07644

Properties of Materials at High Pressures and Temperatures

Francis Birch and Eugene C. Robertson

Table of Contents

	page
Introduction	1
High-pressure gas system	2
Introduction	2
Tapered cylinder	3
Supporting rings	6
Piston	8
Bottom closure	9
Furnace	10
Measurement of pressure and temperature	11
Freezing pressures of nitrogen and argon	14
Polymorphism of minerals	18
High-pressure system with solid medium	20
Appendix	25
Introduction	25
Plastic-elastic treatment of inner cylinder	25
Elementary theory of conical support	29
Effect of discontinuities of load	32
References	
Distribution list	

argon

Introduction

This project originated as a proposal, dated 6 March 1951, for a two-year program of research into methods of combining pressures up to 30,000 kg/cm^2 with temperatures up to 1500°C, with a special interest in studies of polymorphism. It was not found to be feasible to proceed as rapidly as was initially contemplated, and subsequent renewals of the contract, with no additional funds, continued until 30 September 1955. During most of this period, the work was carried out by Dr. Eugene C. Robertson, holding an appointment as Research Fellow in Geophysics.

The original intention was to apply the method of external conical support of the pressure vessel, developed by Professor Bridgman, to a pressure chamber large enough to contain an electrically heated furnace, with an inert gas as the pressure medium. This kind of system has been employed for many years in this laboratory, and it offers the possibility, at least in principle, of good precision of measurement of both pressure and temperature. The extension of the pressure range from the former 100,000 kg/cm^2 to the new 30,000 kg/cm^2 introduces many new problems, however, especially in relation to the gaseous medium required by the high-temperature condition. Bridgman's apparatus, on which the one described below is modeled, made use of a liquid medium, isopentane, which decomposes at moderate temperatures; there appear to be no liquids suitable for the transmission of pressure at high temperatures. The obvious gases are argon and nitrogen, both of which have been used in the present work.

In the spring of 1953, we began to hear reports of the high-pressure synthesis of various minerals by the Norton Company of Worcester, Mass. The details of their arrangements were not given out at first, but it seemed clear that they had employed a solid transmitting medium. Though undesirable for the purpose of measurement, such systems have possibilities going far beyond those of the gaseous system, and we began to explore a few simple arrangements in which the pressure medium was a plastic solid. In December, 1953, a visit to the Norton Company laboratory was arranged, and a very full disclosure of their methods, and a display of synthetic products, was given by Dr. Loring Coes. Two short papers (Coes, 1953, 1955) describe the highly interesting results obtained, at temperatures of 800 to 900°C, and pressures estimated as high as 30,000 to 45,000 bars. These results were most encouraging, in showing that synthesis of these minerals could be achieved, and they directed our attention to the problem of determining the equilibrium relations in the relevant systems. By analogy with other work in which solid media had been used to transmit pressure, we expected that the reported pressures were probably somewhat too high, and thus that these syntheses could perhaps be realized in our system, despite its lower pressure range. This has turned out to be the case, and we have been

able to establish the equilibrium relations for three high-pressure minerals, jadeite, kyanite, and aragonite, and to synthesize the magnesian garnet, pyrope.

All of this work has been subsequently overshadowed by the accomplishments of the General Electric Company, in a considerable extension of the range of both pressure and temperature, and the reliable synthesis of diamonds. It seems likely that some features of their system will be suitable for use in smaller laboratories, and that a new field of research will be opened up when the details of their method become generally available.

The results of the investigations on polymorphism in the system of jadeite composition have been described in a paper which has been submitted for publication to the American Journal of Science. The system sillimanite-kyanite has received further attention since the conclusion of the contract by Dr. S. P. Clark, Jr., and the results are now being prepared for publication. Dr. Clark has also investigated the system calcite-aragonite, and has submitted the results for publication. In addition to these reasonably complete investigations, there are a number of studies which require further work before they become suitable for publication, but of which the present status may be of interest to others engaged in high-pressure work. These preliminary studies are described in the present report, along with many details which have value only for those actively engaged in such experiments.

High-Pressure Gas System

argon N_2

Introduction:

Bridgman (1937) has described a system for producing fluid pressures up to 30,000 kg/cm^2 in a space approximately 1/2 inch in diameter by 6 inches long. The hydrostatic pressure in the interior of the high-pressure chamber is counterbalanced in part by pressure on the external surface, which is given the shape of a cone and forced into heavy supporting rings. This general principle has been followed in the present design, shown schematically in Fig. 1. A heavy frame of plates and tie rods (A) is fitted with two hydraulic rams, B and C. The lower ram, B, has the function of forcing the high-pressure chamber E into the supporting rings, D; B must also support the load produced by the upper ram C on the high-pressure piston. The ram B has an eight-inch diameter, C has a five-inch diameter. Both are supplied with oil pressure from pumps capable of producing pressures of about 20,000 psi. The capacity of ram B at maximum pressure is thus about 500 tons.

Cylinder E has a bore of 3/4 inches and is 10 1/2 inches long. (Fig. 2) The upper 4 inches must be reserved for the travel of

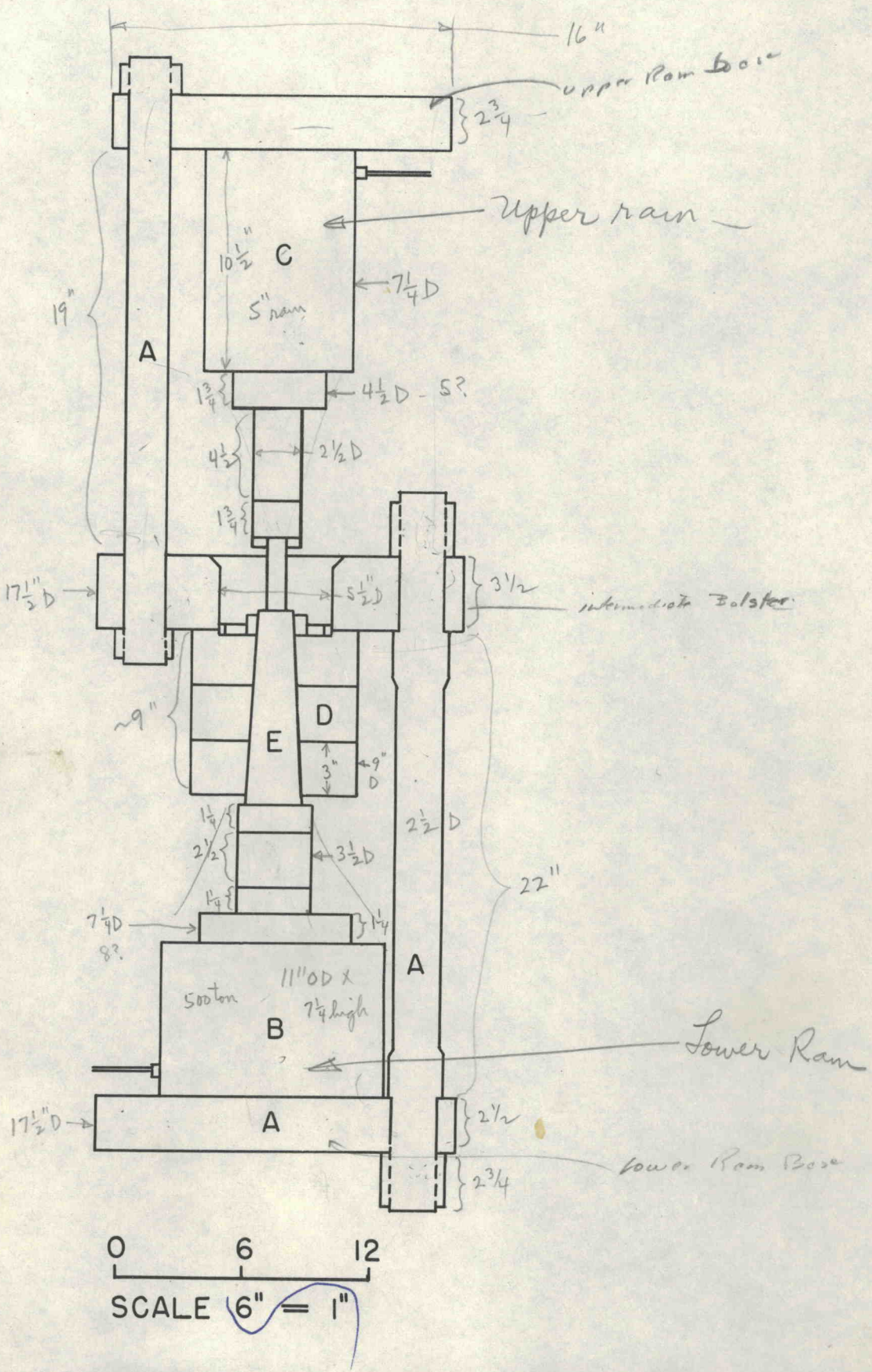

Figure 1. Schematic drawing of pressure-generating system.

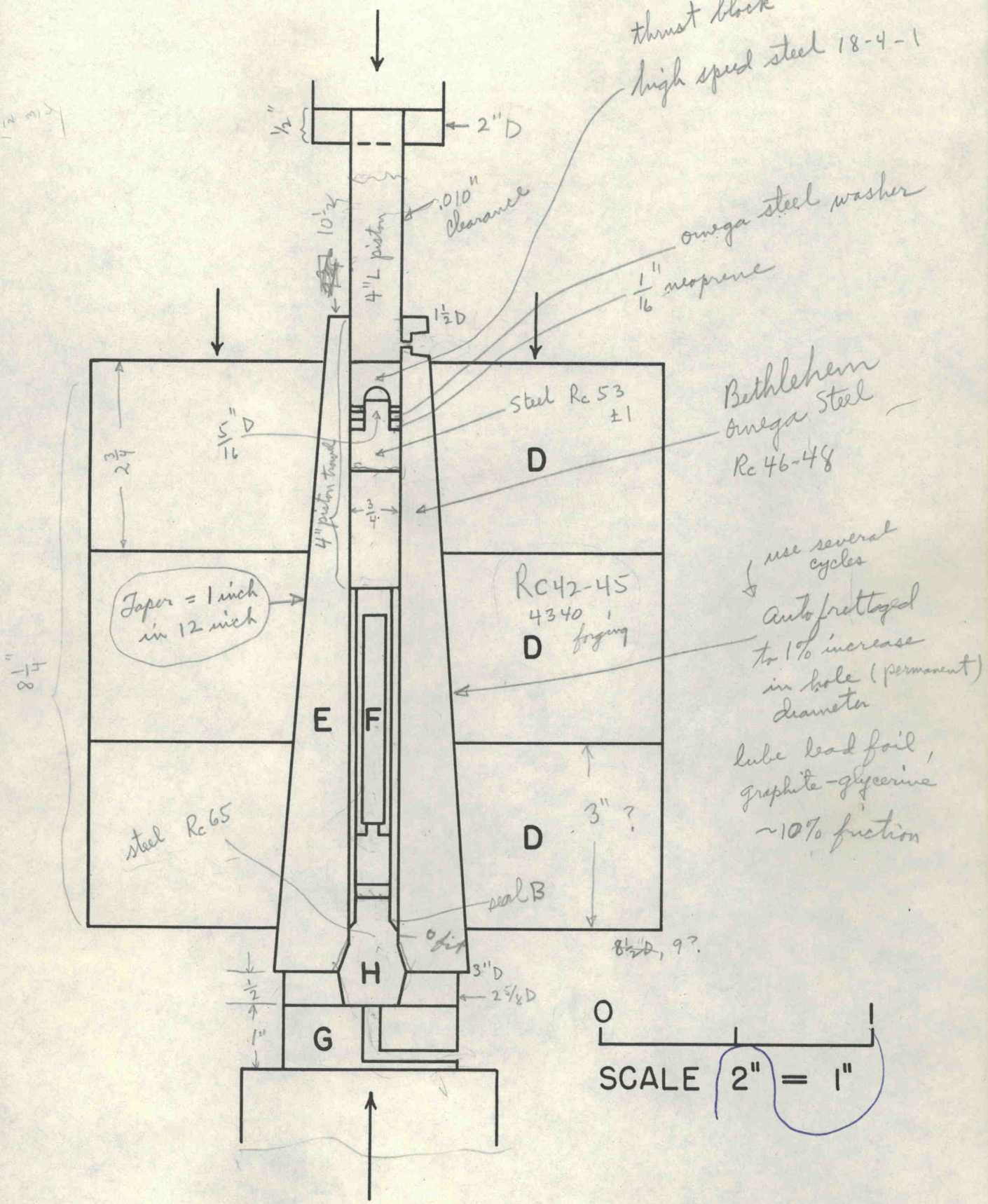

Figure 2. Schematic cross-section of high-pressure system.

the piston; the working space of length 5 inches is normally occupied by a furnace (F), but may of course be used for any purpose. Cylinder E is closed at the base by a plug (H), with packing, carrying insulated electrical leads for heating, and for measurement of pressure and temperature. Two external sizes have been tried for E; in the first design, the diameter was 2 7/8 inches at the base, and the taper one inch in twelve, on the diameter; in the second design, the base diameter was 3 3/8 inches, with the same taper.

Various other parts visible in Figure 2 are the piston, just above E, and thrust blocks above the piston and below E. The piston is of tungsten carbide, with 6% cobalt, the thrust blocks of heat-treated steel; further details are given on the drawings and in Table 2.

Tapered cylinder.

Although failure of nearly every component has taken place at one time or another, the only difficulty for which a reliable solution has not been found is failure of cylinder E. This failure has usually taken the form of a break nearly normal to the axis, a few inches from the upper end, sometimes accompanied by a similar break an inch or so lower. This breakage has been unpredictable; several cylinders have lasted for a large number of exposures to pressures of the order of 20,000 kg/cm^2, others have broken after one such exposure, sometimes at a much lower pressure than the maximum that has been supported. There are two factors which seem to predispose to this kind of failure. First, the internal pressure has a sharp discontinuity at the piston packing; this packing is thin, about 1/16 inch, and below it the pressure may be some 300,000 psi or more, above it, zero. Evidently, the shearing stress must locally reach high values, and several breaks seem to be unmistakably associated with this discontinuity. Second, the longitudinal stress, though compressive, is much lower than either the internal pressure or the external supporting pressure; it reaches a zero value near the free upper end. Thus, the transverse failure is of the nature of a "pinching-off" effect, already familiar in the failure of packed stems and similar components. One modification which appeared to help was to reduce the external support provided by the uppermost ring by enlarging its internal diameter by about 0.010 inch. The internal discontinuity at the piston packing is inherent in this kind of equipment, and not much can be done about it. It does appear, however, that there is an optimum hardness for the cylinder E, at about RC 50; cylinders as hard as RC 55 or so invariably cracked after a short life; below RC 45, the bore enlarges too rapidly, usually with the development of fine cracks but not explosive failure.

Several steels have been tried. Following Bridgman's experience, we started with Bethelehem "Omega", a shock-resisting tool

steel with good hardening characteristics, and this has been used more than any other steel, but with the varying success mentioned above. Another tool steel, Carpenter "RDS", was used for three cylinders; SAE 4340 steel has been used for several cylinders. Some indication of the performance is given in Table 2 but the whole history of each cylinder is probably involved; factors such as amount of external support, duration of pressure, furnace temperatures, etc., may be of some consequence. It seems clear that a combination of high yield stress and ductility in the plastic range is required. As the analysis presented below illustrates, a portion of the cylinder must go beyond the elastic limit, and it is essential that no cracking takes place in this process.

Inadequate metallurgical control is probably to blame for some of the failures. Heat-treating was done at local commercial establishments, which sometimes seemed to be unable to produce the required hardness, or to produce uniform hardness. One result was that over-hard cylinders were often returned for finish grinding, and as hardness increases, the chance of starting cracks in the grinding process itself increases as well. Until a special tapered jig was constructed, it was not possible to obtain satisfactory tests of hardness on the cylinders. It then became evident that many of the fractured cylinders had been much harder than they were intended to be, and that RC50 represented about the optimum value for this piece. But the hardness does not appear to be the only significant factor. It seems probable that carbon percentages above about 0.50 are undesirable even when the steel has been tempered to RC50 or less. Some of the new "ultra-high strength" steels are now under preparation, and hold promise of more reliable behavior.

Table 1

Typical analyses of steels referred to in this report

Name	Manufacturer	C	Mn	Si	Va	Mo	Cr	Ni	W
Omega	Bethlehem	0.55	0.70	2.15	0.20	0.45	-	-	-
Vega	Carpenter	0.70	2.00	0.30	-	1.35	1.00	-	-
RDS	Carpenter	0.75	0.35	0.25	-	-	1.00	1.75	-
High Speed		0.72	0.28	0.22	1.05	-	4.05	-	18.50
SAE 4340		0.40	0.70	0.30	-	0.25	0.80	1.80	-

Table 2

Notes on the service of individual tapered cylinders

No.	Steel	Hardness Rockwell C	No. of exposures	Remarks
2	Omega	51	11	Cracked longitudinally
3	Omega	56-57	3	Short cylinder used with pentane; not ruptured
4	Omega	57	4	Cracked like No. 2
5	Omega	46-50	7	Distorted, not ruptured
6	Vega	57-62	1	Cracked at 25,000 bars, first exposure, with pentane
7	RDS	55-57	3	Cracked at 21,000 bars, third exposure
8	Omega	52	20	Transverse fracture, 1.75 " from small end, joining longitudinal fracture to large end
9	RDS	47-50	21	Breaks similar to those of No. 8
10	Omega	45-46	1	Cracked at 12,000 bars, first exposure
11	Omega	56-57	2	Two transverse fractures, middle piece cracked longitudinally
12	Omega	49	61	Still serviceable
13	Omega	46-47	8	Longitudinal fracture 4.5 " long, beginning at small end
15	Omega	50-52	2	Transverse fracture, 2.75 " from small end, longitudinal fracture to base
16	4340	43-45	9	Not fractured, bore stretched 0.007"
17	Omega	46-48	9	Not fractured, bore stretched 0.005"
18	Omega	47	32	Not fractured, bore stretched 0.008"
24	RDS	46-50	1	Cracked in 3 pieces at 20,000 bars, after 2 hours, first exposure
19L	4340	45	5	Stretched, not fractured
20L	Omega	54-60	1	Three-piece fracture, hardness not uniform
21L	Omega	51	1	Cracked at base by excessive sealing pressure

Note: Cylinders numbered 19L, 20L, 21L were of the larger outside diameter, 2.625 to 3.375 inches.

Supporting rings:

The supporting rings were machined from forgings of SAE 4340 steel, and were approximately 3 inches thick and 9 inches in diameter when finished. After rough machining, the rings were heat-treated to a hardness of Rockwell C 42-45. The flat surfaces and the inner conical holes were finished by grinding. Each ring was then stretched by forcing a conical, hardened mandrel into the conical hole, usually in several cycles of increasing and decreasing pressure, until a permanent increase of hole diameter of roughly 1% was obtained. For this process the surfaces in contact were lubricated with lead foil, graphite and glycerine just as in the normal operation. This autofrettaging raised the effective yield point of the rings well beyond the stresses to be encountered in service, and the subsequent change of dimensions was small. After stretching, the three rings had, of course, to be reground to a common taper.

Figure 3 shows the progressive raising of the yield point for one of these rings; the gauge pressure applied to a 5-inch diameter ram which pushed the mandrel is plotted against the advance of the mandrel into the ring. The first four cycles were carried to progressively higher pressures; the last two cycles were very nearly "elastic", with a very little further stretch, though the maximum pressures were more than twice as great as the pressure required to produce initial yielding. These curves afford an estimate of the friction, which includes that of the 5-inch ram as well as that between mandrel and ring. The difference of pressure between advance and retreat is of the order of 20%, so we may take the curves on advance to be perhaps 10% high, on retreat, 10% low. With this correction, the true pressures can probably be estimated to within 5%.

Figure 4 shows a similar curve obtained when the mandrel was advanced into a complete set of three rings, with essentially elastic response. For a given amount of advance, the pressures are now several times greater than for the single ring, but the frictional effect remains of the same order, - about 10% for the whole difference in this case.

The taper is 1 inch in 12, on the diameter. Thus the advance of the mandrel may be converted by dividing by 12 to apparent increase of hole diameter. The real increase is less than this because of the compression of the mandrel. Without allowing for the finite length of the band of pressure on the mandrel, or for the relatively small axial stress, we may obtain a rough estimate of this compression as follows: let the z-axis coincide with the axis of symmetry and suppose that the effect of the ring may be represented as a uniform radial compression, so that $X_x = Y_y$. Then the strains $e_{xx} = e_{yy} = \frac{(1 - \sigma)}{E} X_x$. For $X_x = 200{,}000$ psi, this gives roughly $e_{xx} = 0.005$; for a 2-inch diameter, the decrease will be 0.010 inches; for a 3-inch diameter, 0.015 inch.

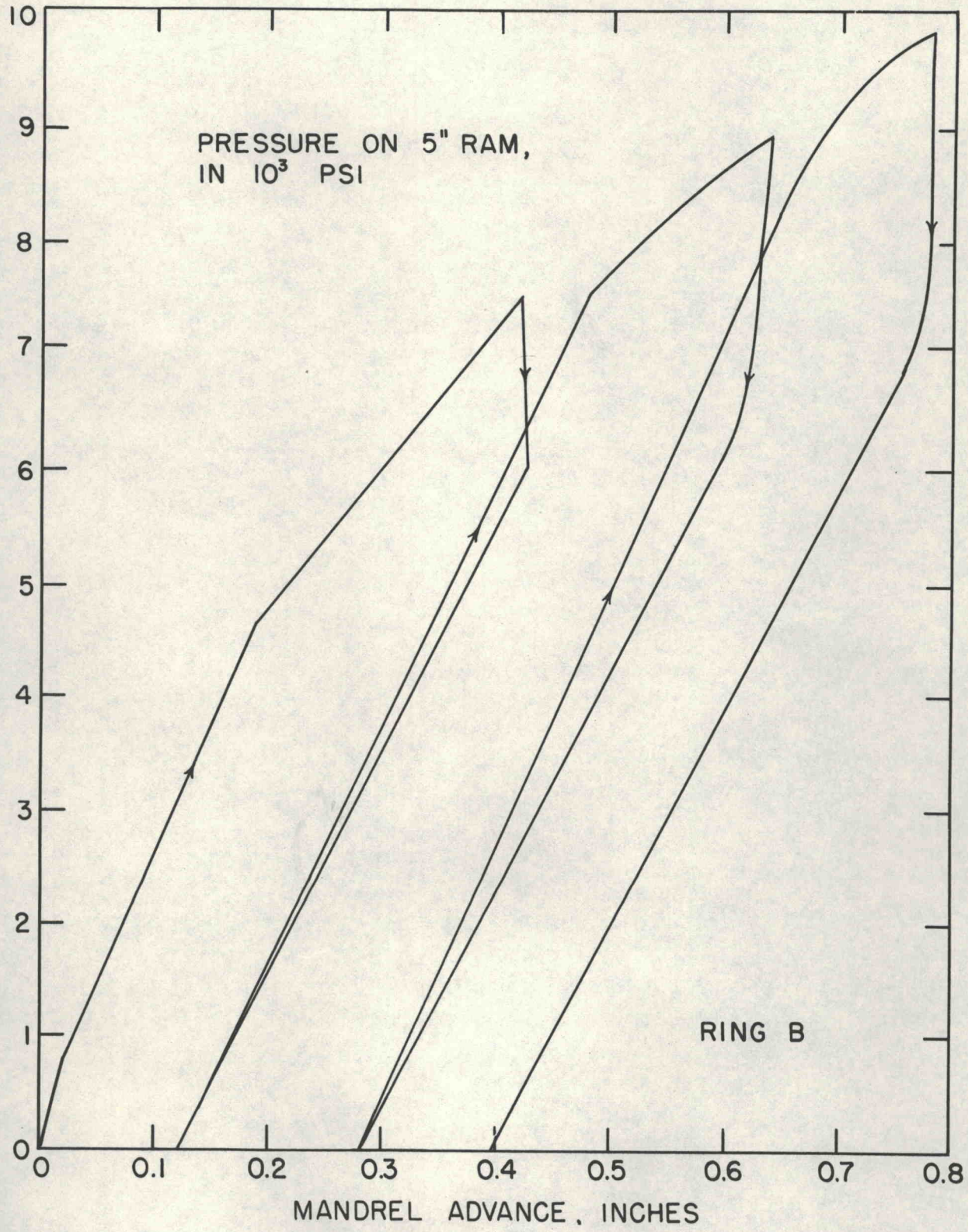

Figure 3. Observations taken during several cycles of stretching of supporting ring B . Pressure on 5-inch diameter ram driving a solid tapered mandrel into the ring , versus the advance of the mandrel .

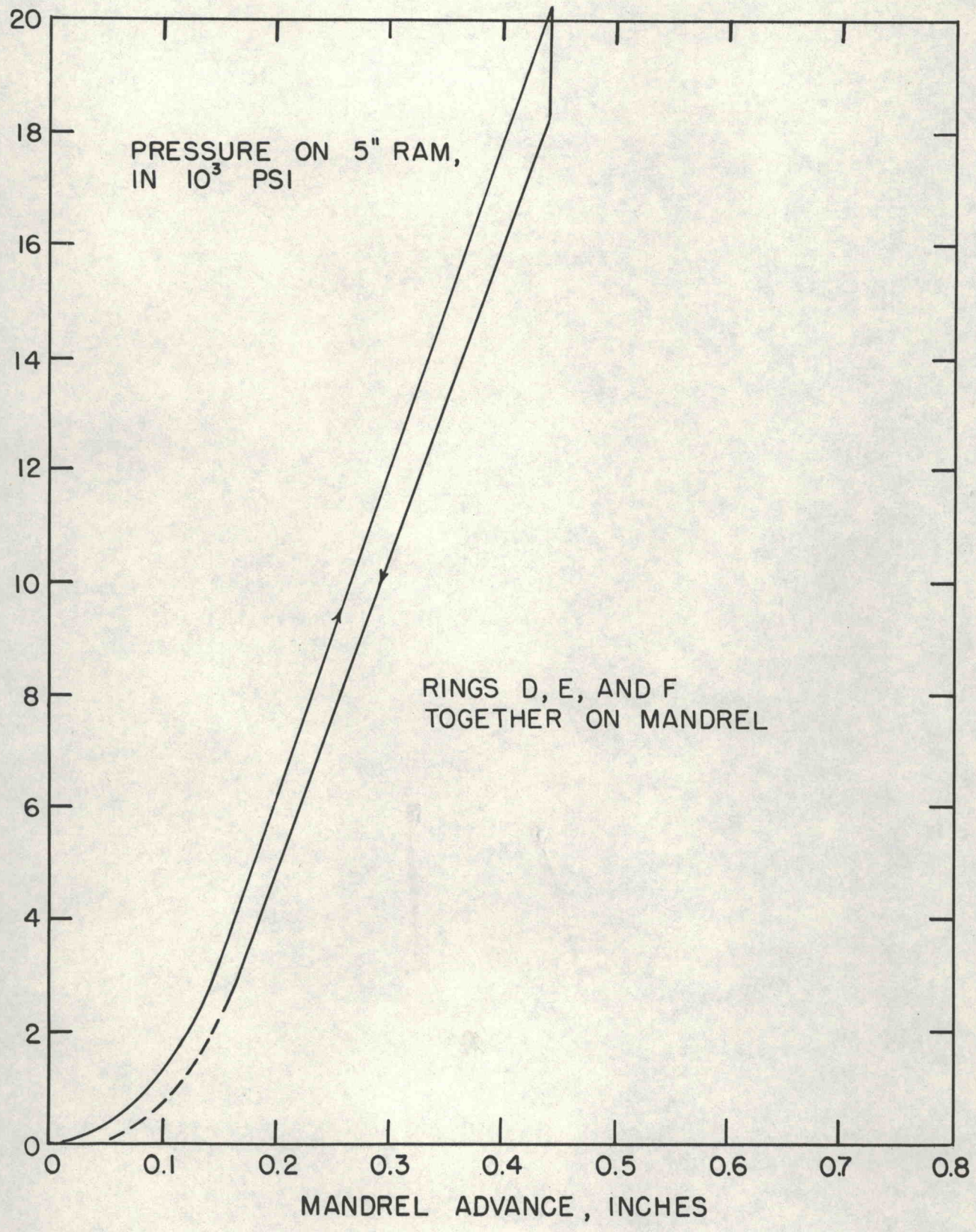

Figure 4. Pressure on 5-inch ram versus mandrel advance, when mandrel was forced into a complete set of supporting rings, D, E and F.

Table 3

Stretch and internal pressures in supporting rings

Ring	Cycle	Internal diameters before cycle, inches		Uncorrected pressures, in 10^3 psi. Yield	Maximum	
A	1	2.000	2.250	90	127	
	2	-	-	130	189	
	3	2.009	2.258	178	217	
	4	2.023	2.268	219	246	
	5	2.033	2.278	-	222	(no yield)
B	1	2.247	2.497	-	97	
	2	-	-	85	159	
	3	2.259	2.505	159	188	
	4	-	-	195	207	
		2.279	2.524			
C	1	2.504	2.755	80	138	
	2	-	-	159	174	
	3	-	-	173	190	
D	1	1.996	2.245	130	179	
	2	2.004	2.253	170	219	
	3	2.011	2.263	200	226	
		2.026	2.277			
E	1	2.244	2.495	93	150	
	2	2.256	2.507	158	195	
	3	2.268	2.519	200	220	
		2.275	2.524			
F	1	2.498	2.749	152	175	) Friction
	2	2.511	2.760	169	207	) high
	3	2.524	2.770	180	218	)
		2.538	2.788			

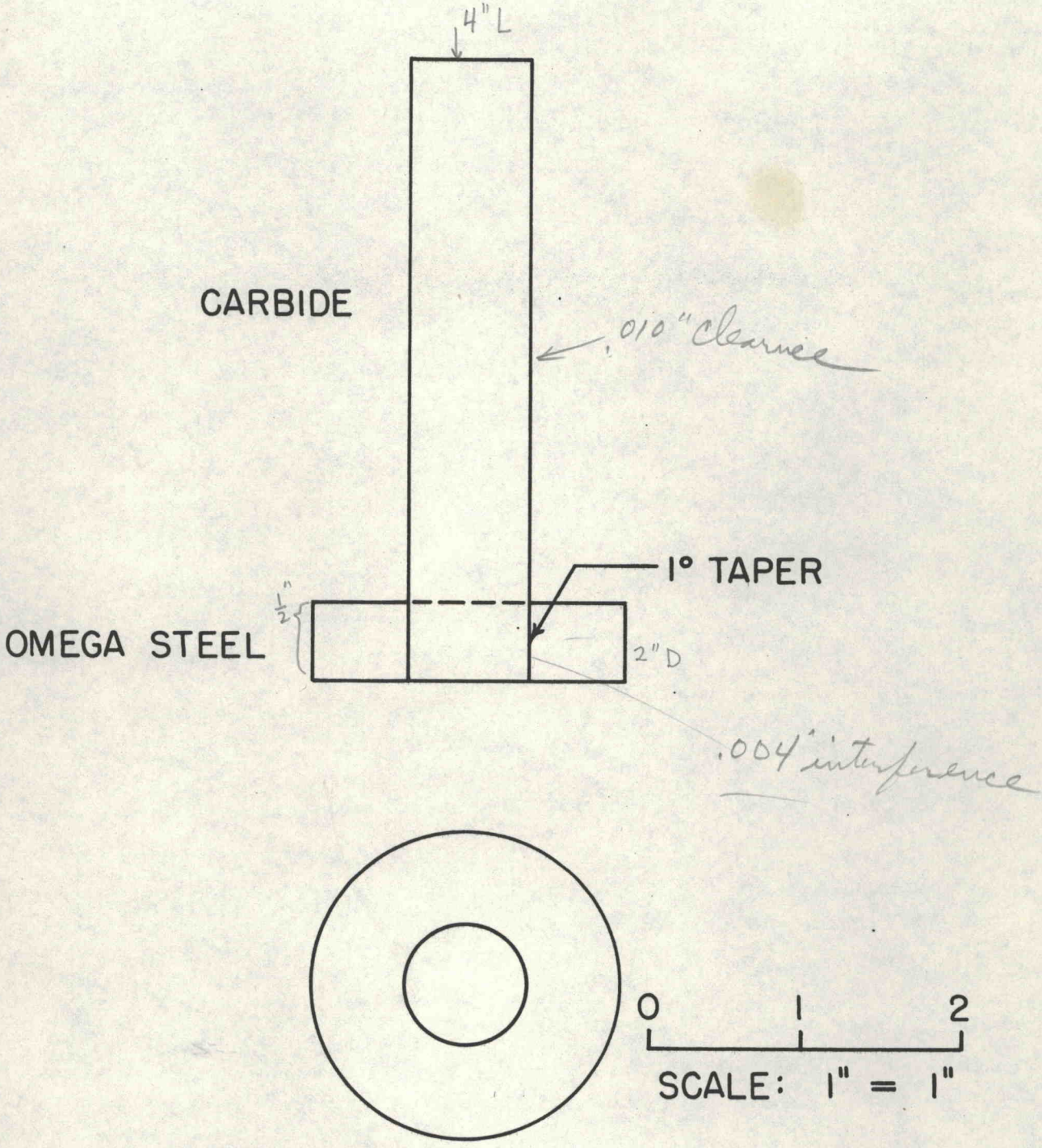

Figure 5. Details of high-pressure piston .

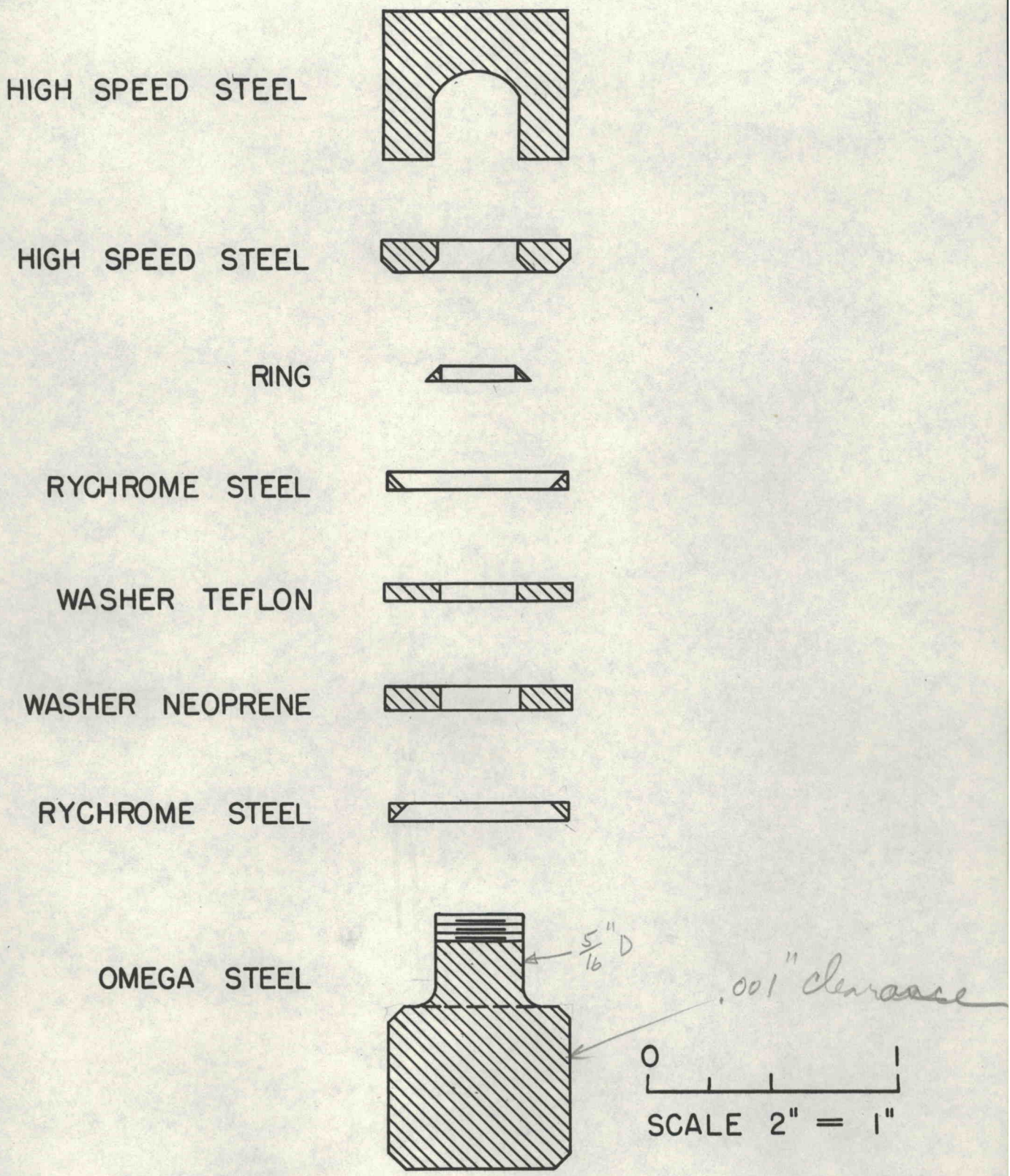

Figure 6. Details of high-pressure moving plug.

stem of the mushroom to pinch off. Thus, if 1/4 of the whole area were unsupported, - the usual ratio in low-pressure design, - the compressive stress in the annular part of the thrust block would be 4/3 times the internal pressure, or 600,000 psi if the pressure were 450,000 psi. This is unduly high for steel. The first packings were made, therefore, with a stem of 1/4 inch diameter, thus 1/9 of the area, so that the multiplication factor for the pressure in the thrust block was 9/8. This appeared to be statisfactory with regard to strength, but the sealing pressure was not sufficient. The mushroom stem was then increased to 5/16 inch, and this has been used for most of the work with little trouble from mechanical failure.

On the other hand, a series of baffling leaks was encountered at the moving packing which led to a number of trials of various materials and arrangements until the reason was finally discovered. The explanation appears to be as follows: New fresh samples of neoprene packing (Garlock 7986) are satisfactory, but after a matter of several months, an aging process seems to occur which causes this material to crack when used at high pressure. Some improvement was obtained by the use of a thin lead washer behind the neoprene, but the best solution appears to be to get a fresh batch of packing. In certain respects, high pressures produce effects resembling those of low temperature, and the embrittlement of rubbers at low temperatures is well known. Silicone rubber might be an improvement if it could be made with sufficient mechanical strength; presently available grades do not seem to be satisfactory.

A superior material for this purpose, according to Professor Bridgman, is a synthetic rubber made by DuPont, called "Adiprene". Samples of this were used by him for runs to 30,000 bars, with pentane, the same washer lasting for repeated use. Apparently this material was made only as a laboratory curiosity, and no more has ever become available.

Bottom closure:

The bottom closure has the function of sealing the lower end of the tapered cylinder, and also of providing for pressure-tight, insulated electrical connections between the furnace winding, thermocouples, and pressure gauge and the external circuits. It was anticipated that this might be a source of much difficulty, but happily this was not the case. A slightly enlarged version of the closure used by Bridgman for liquids has been relatively free from trouble; the only inconvenient feature has been the necessity for frequent renewal of the metal packing rings.

The general arrangement is shown in Figure 7. The body of the piece is made of high speed steel, hardened and drawn to RC 65. The lower part was tapered outward to give a larger area of

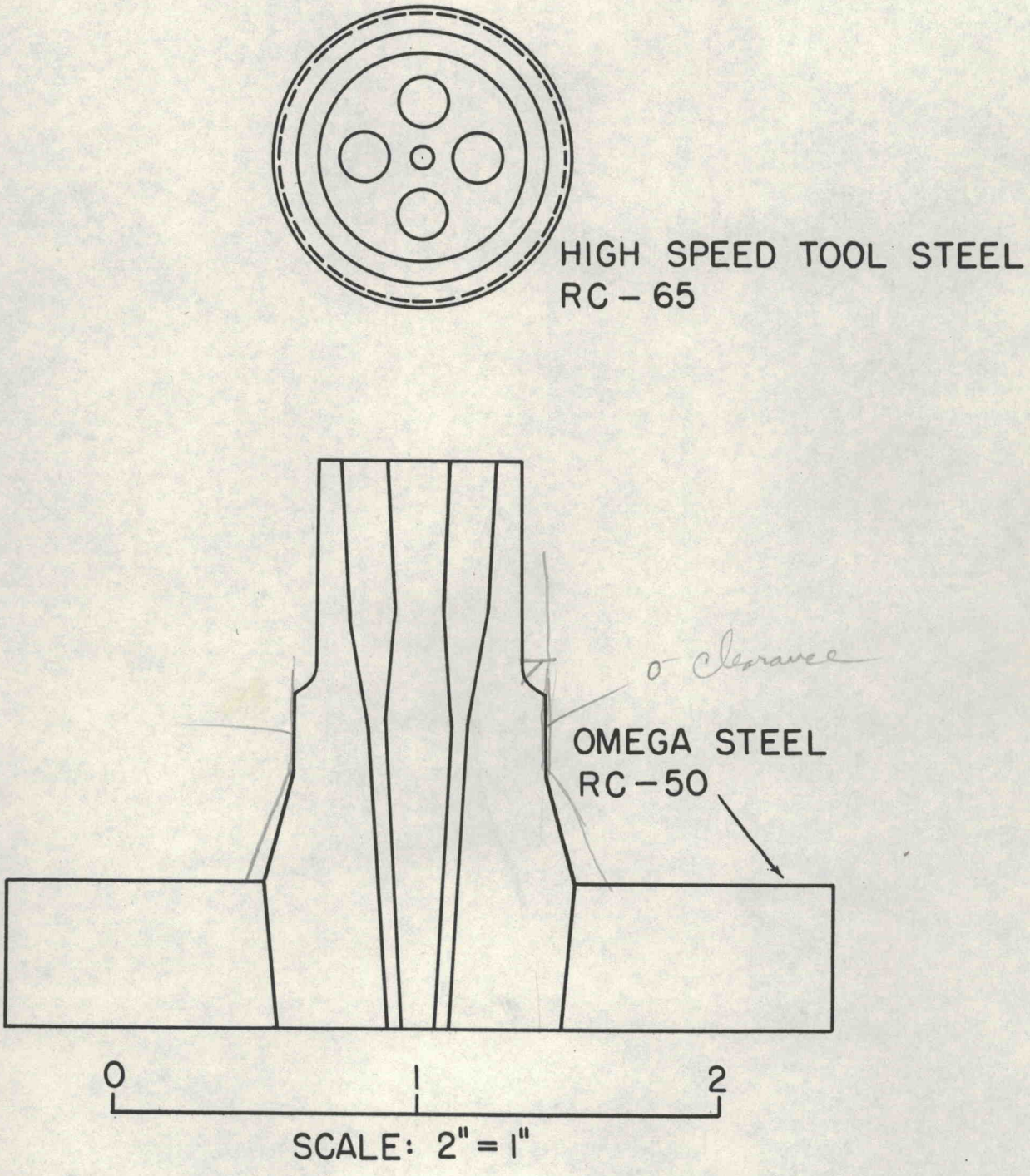

Figure 7. Details of bottom closure with four terminals .

support, after the failure of a straight piece, and cylinder E is correspondingly enlarged so that no contact takes place except at the packing rings. The width of the packing is adjusted so that the initial compression on forcing the flat ring against the end of cylinder E provides a seal; as the pressure builds up, the seal is obtained between the double steel ring and the curved exterior of the closure. The inconvenience of this arrangement is that after a high-pressure run, the steel rings may fill the space and leave no unsupported area for the next time; even if this does not occur, it often happens that this packing will leak on the second or third run.

Because of this, some work has been done with a mushroom-type of lower closure. This appears to be feasible up to about 20,000 bars or a little more; the stem was "pinched off" at about 25,000 bars. With a little further work, it may be possible to raise the working range of this much more satisfactory kind of closure very nearly to that of the cylinders.

The electrical connections were made through hardened steel (drill rod) cones insulated by thin conical sleeves of pipestone or its commercial equivalent, "Lava", or massive, fine-grained pyrophyllite. The wires attached to these cones are free from stress and may be of any desired material, such as platinum or platinum-rhodium alloy for thermocouple extension leads. Five separate leads have been successfully introduced; a six-terminal plug cracked in hardening, but might be produced with more careful handling. The various small parts included in the packing are shown in Figure 8. An arrangement found very convenient was the use of a miniature socket, similar to the base of a miniature vacuum tube, indexed to plug into prongs extending upward from the conductors in the bottom closure. This socket was attached to the furnace tube, and made it possible to disengage and remove the furnace through the upper end of the cylinder without disturbing the bottom closure or its various supporting pieces, or the external electrical connections.

Furnace.

The details of furnace design were varied considerably in efforts to prolong the life of windings, improve the temperature distribution, and facilitate loading and unloading. For temperatures below about 1000° C, the bore was usually 1/4 inch, the furnace tube of porcelain with an outer diameter of 5/16 inch, and the length of winding, of nichrome or kanthal ribbon, about three inches (Figure 9). For higher temperatures, a platinum-rhodium alloy was wound on tubes of porcelain or alumina, with a smaller bore, approximately 1/8 inch, and the same length. The space between the winding and the furnace container, a steel or later, copper tube, was filled by a sleeve of "Lava" or porcelain. Within the furnace bore was a multibore porcelain tube carrying thermocouples; the charge was placed between two

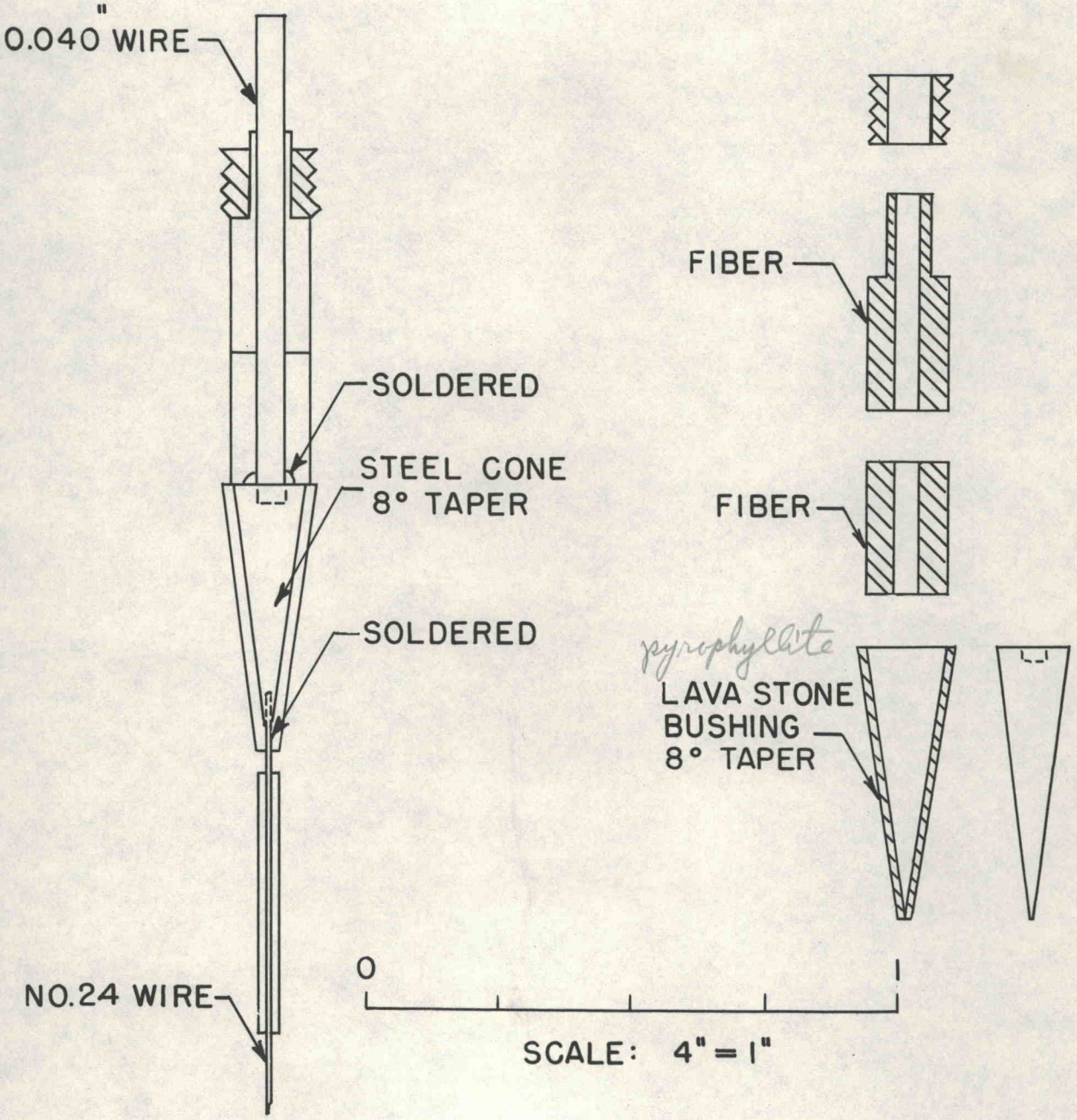

Figure.8. Details of insulated conductors.

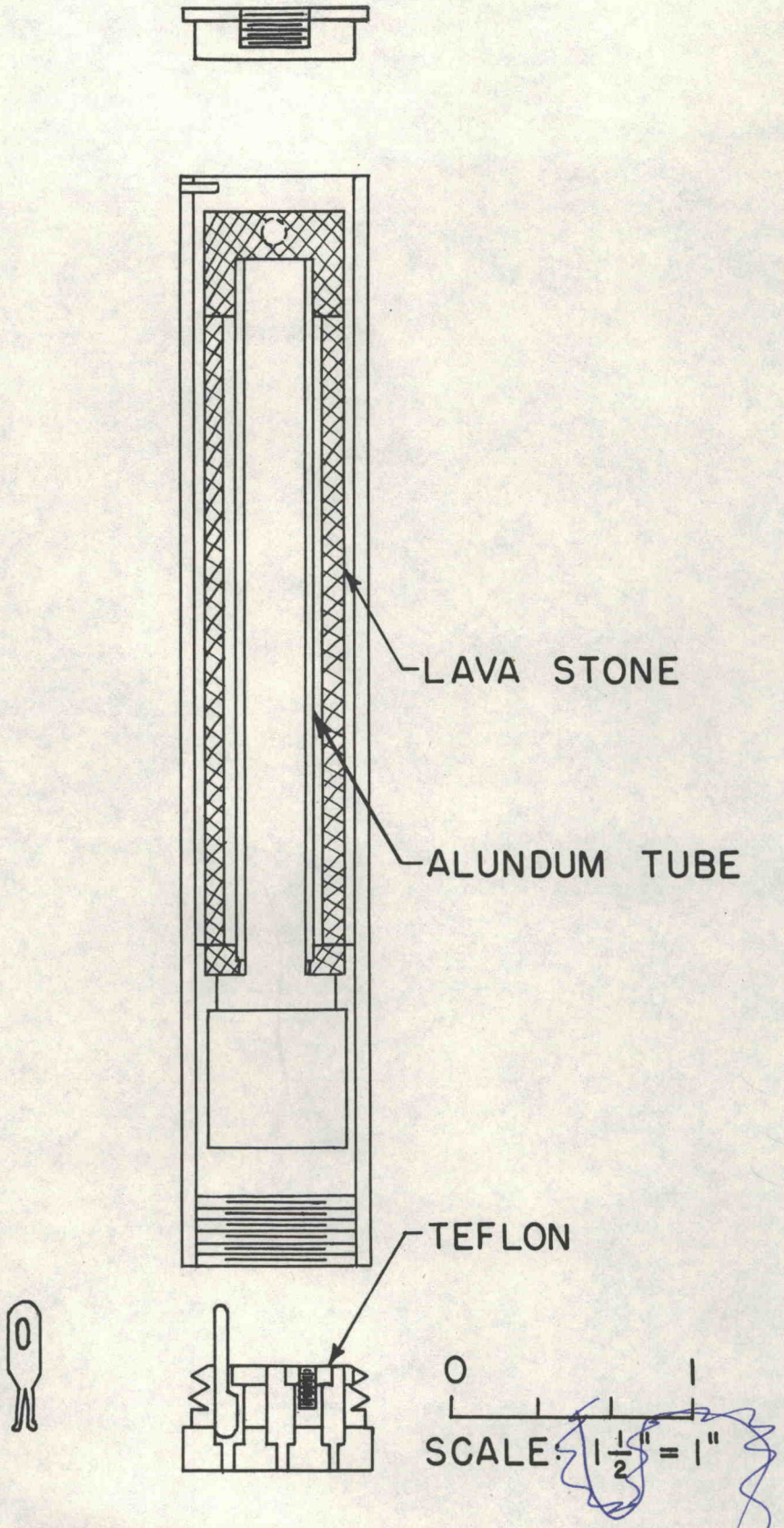

Figure 9. Details of typical furnace .

thermocouple junctions. The upper part of the furnace was closed by a solid plug, and all interior space filled with powdered alumina or magnesia in order to reduce convection. One end of the furnace winding was grounded to the furnace container; the other end was connected, either by soldering or through a connector, to one of the insulated conductors in the bottom closure. The thermocouple wires were similarly connected to individual leads in the bottom closure. At the base of the furnace tube, or in an improved model due to Dr. Clark, on the bottom closure itself, is mounted the manganin coil which serves as pressure gauge.

The winding was usually designed to have a hot resistance of about 13 ohms; the power input was controlled by a variable transformer supplied by a constant voltage transformer with a capacity of 1 KVA. The maximum current from the 115 volt supply was thus about 9 amperes. Control of temperature was manual for most of this work, as it was feared that control by the common "on-off" type of control would produce undesirable large fluctuations in the temperature of a system having so small a thermal mass. This feature was of value for quenching experiments, when it was desired to reduce the temperature as quickly as possible to a point at which reactions would be effectively terminated, perhaps several hundred degrees. On switching off the power, the temperature fell, in a matter of 20 to 30 seconds, very nearly to the temperature of the steel cylinder, which never exceeds about 100°C. Later it was found, however, that by passing a small fraction of the total current through the switch of a Minneapolis-Honeywell "pulse-type" Pyr-o-vane controller, with a shunt carrying the main current, a very satisfactory control could be obtained.

In so small a furnace, it is difficult to produce more than a short region of relatively uniform temperature. Since the ends of the furnace are at about 100°C, and the hottest point may reach 1400°C or so, a few centimeters away longitudinally, and less than 1 cm radially, the gradients are bound to be high. There must be a point of maximum temperature along the tube, and by flattening this maximum by varying the pitch of the winding or by introducing a solid conductor, a useful space perhaps 1 cm long with a relatively well-defined temperature can be established. The variation of temperature between the ends of the charge was measured by the two thermocouple junctions which bracketed this region. The best position was found by trial; it usually appeared to be slightly above the center of the winding, as might be anticipated.

Measurement of pressure and temperature.

Though rough measurements of pressure may always be made from the ratio of areas of piston and ram and the pressure on the ram, the uncertainties resulting from friction and distortions

may be large, and the pressures given in this work depend upon the change of electrical resistance of a manganin coil exposed to gas pressure. The high-pressure scale depends upon fixed points established by Bridgman (1940), of which we have used the freezing pressure of mercury, 7640 kg/cm^2 at 0°C and 12,000 kg/cm^2 at 22°C, and the transition pressure for the bismuth modification I to II, 25,800 kg/cm^2 at 22°C. [The unit of pressure for the experimental work is the kg/cm^2, which equals 0.98 bar; the difference between these two units is of no consequence for the present work.] These pressures are probably accurate to about one part per thousand. With the aid of these fixed points, Bridgman has shown that the resistance of manganin wire is not quite linear with pressure: if the coefficient of a manganin coil is determined at the freezing point of mercury, and then used, by linear extrapolation, to measure the bismuth transition pressure, the error is about two percent. This would not be a significant error for the present work; it can, moreover, be eliminated by the use of a second-degree relation between resistance and pressure. The principal uncertainty of pressure measurement in this work arises from the effect of temperature upon the resistance of the manganin gauge coil.

Between 20° and 30°C, the resistance of manganin passes through a flat maximum with respect to temperature, and in ordinary installations of manganin pressure gauges it is rarely necessary to correct for small changes of ambient temperature. In the present system, however, the gauge may reach temperatures as high as 100°C, which depend upon the power input and the duration of heating. As the coil temperature rises at constant pressure, its resistance decreases, giving the appearance of a drop in pressure. It became necessary to determine the temperature of the coil, and also to examine the effect of temperature upon the resistance-pressure characteristic of manganin.

The pressure gauges were 50-ohm coils of No. 40, double-nylon-covered manganin wire recently obtained from the Driver-Harris Company, wound non-inductively on Teflon spools and protected by Teflon sleeves. The sensitivity of resistance measurement corresponded to a pressure difference of 10 kg/cm^2. A number of these coils were calibrated against the freezing point of mercury at 0°C at various times; the pressure coefficient is $2.31 \cdot 10^{-6}$ per kg/cm^2 at room temperature, with variations of about one-half percent. (coils made of enameled manganin wire obtained from the same manufacturer about twenty years ago show a coefficient of about $2.5 \cdot 10^{-6}$ per kg/cm^2.) Several coils were then heated to temperatures up to about 125° at one atmosphere, and also at 7500 kg/cm^2, measurements of resistance being taken as function of both temperature and pressure. The results are summarized in Table 4. The effect of temperature is slightly smaller at 7500 kg/cm^2 than at 1 atmosphere, with the corollary that the pressure coefficient is slightly larger at 100°C than at 25°. The effect of changing the temperature, at constant pressure, from 25°C to 100°C is

equivalent to a pressure change of approximately 900 kg/cm^2. An error in the temperature of the coil of 5°C at 100°C is equivalent to a pressure change of roughly 100 kg/cm^2. The cumulative errors may amount to as much as several hundred kg/cm^2 at the highest pressures.

Table 4

Effect of temperature on the electrical resistance and pressure coefficient of resistance of manganin

t°C	R/R_{25}	Increase of pressure coefficient, percent
25	1.0000	0
50	0.9998	-
75	0.9991	0.8_1
100	0.9979	1.6_7
125	0.9965	2.7_7

For comparison with Table 4, Bridgman (1938, p. 170) gives an increase of coefficient of 0.6% between 30°C and 75°C; an earlier and probably less satisfactory determination (Bridgman, 1935[a], p. 79) gives an increase of 1.3% between 0 and 50°C, 2.0% between 0 and 95°C: There is some evidence that the temperature coefficient of the pressure coefficient is more variable than the pressure coefficient itself.

The temperature of the pressure gauge in our high-pressure system was obtained from the change of resistance of a copper coil mounted close to the pressure coil and having the same external dimensions; it was supposed, for this correction, that the slope of the resistance-temperature curve of copper is unaffected by pressure, in accordance with Bridgman's determination (1931, p. 262; 1938, p. 174) of the small effect of temperature upon pressure coefficient. A rough value of the coil temperature may also be obtained from the temperature of the base of the tapered cylinder.

Temperatures in the furnace were determined by thermocouples, usually with at least two junctions close to the charges. The temperature is far from uniform as mentioned above. By placing the charges between two thermocouple junctions, we attempted to bracket the actual temperature, but the uncertainty remains appreciable.

Chromel-alumel couples were first used, with leads of chromel and alumel through the packing of the bottom closure to

an external cold junction. The effect of pressure on the thermal emf of this couple has been shown to be negligible up to 4000 kg/cm^2 and 600°C (Birch, 1939); the pressure has been extended to 7000 kg/cm^2 in unpublished work. It has been assumed that the pressure effect is still relatively unimportant at the higher pressures of the present study. Under ordinary conditions, the chromel-alumel couple may be used to some 1100-1200°C, but there is evidence of some kind of deterioration in high-pressure nitrogen at temperatures of 900°C and higher. This became noticeable as an apparent decrease of temperature at constant power input and constant pressure, and it has been tentatively ascribed to nitriding of the alumel wire. The effect disappeared when platinum-platinum-10% rhodium couples were substituted for chromel-alumel. A pressure effect has been noted for this couple, amounting to an apparent decrease of about 12°C for 20,000 kg/cm^2 and 1000°C on linear extrapolation from the measurements at lower temperatures and pressures (Birch, 1939). A further uncertainty was introduced by the use, with this couple, of copper leads through the bottom closure. This made the connection from couple to copper inside the pressure chamber the effective cold junction, for which the temperature was taken as equal to that of the copper coil described above. This particular correction has been eliminated in later work by the use of platinum and platinum-rhodium leads through the packing. The major uncertainty as to temperature arises from non-uniformity of the temperature distribution, as mentioned above.

Freezing pressure of nitrogen and argon.

The freezing curves of argon and nitrogen have been followed to high pressures by a number of investigators, though no one has hitherto observed the freezing of these substances at temperatures as high as room temperature. Empirical curves of various types have been used to represent the experimental data, and while satisfactory for this purpose, they are of questionable value for extrapolation far beyond the range of measurement. Probably the most satisfactory form of equation is that of Simon (1937), for which some theoretical justification has recently been given by Domb (1951) and by Salter (1954). Simon's formula may be written in the form, $P/P_o = (T/T_o)^c - 1$ where T_o is the freezing temperature (absolute) at 1 atmosphere (the "normal" freezing or melting point), c a numerical constant, P_o a constant having the dimensions of pressure, and P the freezing pressure at the absolute temperature T. P is the "gauge" pressure, that is, the excess of pressure above 1 atmosphere; at pressures of the order of 1,000 atmospheres or more, this distinction is unimportant.

The experimental data comprise the measurements by Simon, Ruhemann and Edwards (1929,1930) to 5,000 atmospheres, by Bridgman (1935) to 6,000 kg/cm^2, and of Robinson (1954) to about 9,000 atmospheres, for both nitrogen and argon; and by

Benedict (1937) to 6,000 kg/cm^2 and by Mills and Grilly (1955) to 3,500 kg/cm^2, for nitrogen only. The data of these authors have been used to find the freezing pressure at 20°C, which is,

Table 5

Measured and calculated freezing pressures for nitrogen and argon, for Bridgman's data.

Pressure, kg/cm^2		
Measured	Calculated	
	Nitrogen	Argon
1000	994	1000
2000	2002	1994
3000	3011	3010
4000	3993	4009
5000	4992	4995
6000	6010	5983

28,300 ats freeze nitrogen at 20°C

13,000 ats for A at rm temp

of course, well beyond the range of their observations. A Simon formula has been fitted for this purpose to each of Bridgman's sets of data; the calculated pressures for each material are shown in Table 5. Though these are not least-squares solutions, it is unlikely that the fit can be significantly improved. The measurements of Bridgman, Benedict, and Mills and Grilly for nitrogen are in extremely close agreement, and all give about 24,000 kg/cm^2 for the extrapolated freezing pressure at 20°C. Robinson's measurements cover the greatest range of pressure, and the extrapolated freezing pressure at 20°C is about 26,000 kg/cm^2. The best observed value obtained by Robertson, by the method described below, is 28,300 kg/cm^2.

There are fewer measurements for argon, but as the freezing temperatures are higher, the observations come closer to room temperature and much less extrapolation is requred. The calculated values fall between about 12,000 and 13,600 kg/cm^2; the best observed value is 13,000 kg/cm^2.

The occurrence of freezing in our apparatus is shown by several effects. First, there is an increase of friction associated with the advance of the piston, often accompanied by "abnormal" sounds of squeaking or crunching; second, if the piston continues to advance, the pressure remains nearly constant, as more gas freezes out; finally, if the advance is continued sufficiently, failures begin to take place in the electrical circuits, as the solidified medium pushes or drags various wires out of position. When the internal furnace is turned on, the mean temperature of the gas is, of course, increased, and freezing

Table 6

Freezing pressure at 20°C

Extrapolation, except as noted, by Simon's formula: $P/P_o = (T/T_o)^c - 1$. The constants P_o and c are tabulated below. T_o is the freezing temperature (Kelvin) at one atmosphere.

	P_o kg/cm^2	c	T_o deg.Kelvin	P (20°C) kg/cm^2
Nitrogen				
By extrapolation				
Simon, Ruhemann, Edwards (1930)	1250	2.203	63.2	35,460
Bridgman (1935)	1650	1.787	63.2	23,950
Benedict (1937)	1660	1.78152	63.21	23,850
Robinson (1954)	1860	1.775	63.7*	26,070
			63.2	26,400
Mills and Grilly (1955)	1638.3	1.791000	63.16	23,960
Observed, Robertson (1954)				28,300 ± 300
Argon				
By extrapolation				
Simon, Ruhemann, Edwards (1930)	3000	1.288	83.4	12,100
Bridgman (1935)	2200	1.578	83.9	13,640
Robinson (1954)	3616	1.16	83.2	11,960
Observed, Robertson (1954)				13,000 ± 100

Note: Another formula given by Benedict, $P = 21,306 + 155.12\ t + 0.25557\ t^2$, where t is the centigrade temperature, gives $P = 24,510$ kg/cm^2 for $t = 20°C$.

* This figure is given in the paper; if this is a misprint for 63.2 K, the second pressure is relevant.

requires somewhat higher pressure, but this is determined mainly by the temperature of the steel walls of the cylinder which will be the coolest part of the system. In order to freeze, the gas must lose its latent heat; freezing begins on the cylinder walls, which usually do not get above about 50°C. Once a film of frozen argon or nitrogen is formed on the walls, it becomes increasingly difficult for heat loss to occur, since these solids are poor conductors of heat; while the initiation of freezing is relatively easy to detect, thereafter the system departs more and more from equilibrium, the gas becomes "under-cooled" or "over-compressed", and it is difficult to observe the reversal of the reaction. Thus, though the freezing interferes with the proper functioning of the internal electrical arrangements, the present system is not well-adapted to give accurate measurements of the freezing pressures.

This interpretation is confirmed by observations on the freezing of carbon dioxide, for which the freezing curve has been followed to 93.5°C and 12,000 kg/cm^2 by Bridgman (1931). At room temperature, the freezing pressure given by Bridgman is about 4800 kg/cm^2; the characteristic freezing phenomena began in our apparatus at roughly 5000 kg/cm^2, but no effort was made to obtain a more exact determination.

The best determinations, still very rough, were obtained with an arrangement resembling in principle the method of the "blocked capillary". In place of the usual furnace, there was introduced a steel plug 4 inches long with an axial hole about 1/8 inch in diameter. One manganin pressure coil was placed on the upper end of this plug, with its connecting leads passing through the hole in a double-bore porcelain tube which closely fitted the hole in the steel plug; a second coil was connected in the usual place at the bottom. As freezing began, solid was formed in the small annular space between this plug and the cylinder, and in the capillary hole, these being the places where heat can be most easily lost. Once the spaces were filled with solid, a difference of pressure began to be shown between the two gauges on further advance of the piston, the bottom one giving the equilibrium pressure, the upper one a higher, non-equilibrium pressure. This arrangement was successfully employed for one observation with argon, and for one with nitrogen. The upper coil was eventually disconnected by the breaking of the wire in the capillary hole, and crushed by a plug of solid. The values so obtained are shown in Table 6. It is difficult to set reliable limits for the uncertainty, but it seems probable that these figures are more nearly correct than those obtained by extrapolation from the lower pressures. For our purpose, the principal conclusions are that nitrogen is a suitable medium for our whole pressure range, while argon can be used to about 16,000 if the cylinder walls are kept at 50°C, to 20,000 kg/cm^2 if they are kept at 100°C. As both are relatively weak solids, they may be of use in the solid form in other types of pressure equipment.

Polymorphism of minerals.

Since the principal purpose of this work was the study of high pressure polymorphism of minerals, a summary of the results of this kind is included, although separate reports of the various systems are to be published and should be consulted for details. (Robertson, Birch and MacDonald, 1957; Clark, Robertson and Birch, 1957; Clark, 1957.) It should be understood that the requirement of high pressures for the formation of certain minerals in the laboratory does not necessarily mean that high pressures are required in nature. In the systems which have been studied, the slopes of the equilibrium curves, dT/dP, are positive. High pressures are required in order to study these systems at temperatures at which the reactions proceed with sufficient rapidity for laboratory purposes. This means that there must be an appreciable conversion of the starting material to another crystalline modification in a matter of hours. The reaction rates can sometimes be greatly increased by the use of catalysts or "mineralizers", but for the study of equilibrium relations it is desirable to keep the chemistry as simple as possible, since the quantities available are usually inadequate for chemical analysis. Identification of phases depends partly upon optical properties, but mainly upon the X-ray diffraction patterns. Neither of these methods is sensitive to compositional differences which may conceivably affect the position of the equilibrium curve. Small amounts of water have been used in most of our systems, on the assumption that water does not appear in the final products and hence does not affect the equilibrium. This assumption is difficult to verify, and while it may be approximately correct for low partial pressures of water, it may be less true for high water pressures.

The lowest temperatures at which reactions can be observed are different for the different systems. The calcite-aragonite reaction can be followed down to about 375°C, the jadeite - albite + nepheline reaction to about 600°C, the kyanite-sillimanite reaction to about 1000°C. The last-named reaction involves two exceedingly refractory minerals, which are fairly common, however, in metamorphic rocks where the temperature of formation must have been considerably lower than 1000°C. It seems likely that the natural reactions have the assistance, not only of relatively long periods of time, but also of shear stresses, which the recent work of Griggs and Kennedy (1956) shows to be highly effective in accelerating reactions of this kind.

The general technique is as follows: the charge which is to react is first enclosed in a thin capsule of gold or platinum; this is placed between the two junctions of the thermocouples in the furnace, which is in turn seated in the pressure chamber. The pressure is then raised almost to the desired value, the temperature brought up rather rapidly to the desired value and the pressure readjusted as required. Conditions are held as steady as possible for the duration of the run; at the end, the

current is turned off, the temperature drops rapidly while the pressure decreases slightly, and the charge is "quenched" under pressure to the temperature of the steel container within a minute or so. This quench might not be sufficiently rapid for some purposes, such as studying crystallization from a melt of low viscosity, but it appears to be suitable for studying the very sluggish solid-solid transitions of this work, as well as the crystallization in feldspar melts or in fused jadeite.

The equilibrium curve is approached as the limiting line, on one side of which phase A, say, is converted, or begins to be converted to phase B, while on the other side, phase B begins to be converted to phase A. It is important to demonstrate that reversibility does hold across the line, although in practice it may be difficult to place well-established experimental points as close to the imaginary line as one would like. In part this is due to the effect of temperature gradients, in part to the sluggishness of the reactions. In some systems, as in the jadeite - albite + nepheline system, it is convenient to start with glass of the proper composition and to study the crystalline products. In others, glass cannot be readily prepared, but a fine-grained crystalline starting material may be formed by decomposition of a hydrated mineral; thus, kaolinite was the starting material for many of the runs in the sillimanite-kyanite system. The kaolinite breaks down to fine quartz and corundum, a refractory mixture which often refuses to be converted further.

Figure 10 shows the equilibrium curves which have been established so far. The work on the system kyanite-sillimanite was partly, and that on calcite-aragonite wholly due to Dr. Sydney P. Clark, Jr., continuing with the equipment after the expiration of the contract period. The line for the calcite-aragonite equilibrium is shown prolonged to meet the low-pressure curve determined by Jamieson (1953) from the study of electrical conductivity in solutions. The high-pressure points are evidently consistent with this low-pressure work. The pressures are about 1300 bars higher than those found by MacDonald using the method of Griggs and Kennedy (MacDonald, 1956).

In addition to these relatively complete studies, a few preliminary results are available on the synthesis of the magnesian garnet, pyrope, $3MgO \cdot Al_2O_3 \cdot 3SiO_2$. This was crystallized from a glass of this composition under the conditions shown in Table 7. The equilibrium relations with the other set of minerals which formed more frequently, forsterite plus spinel plus cordierite, are not yet known; the appearance of pyrope was capricious, the same conditions yielding sometime pyrope, more often the mineral assemblage mentioned above. Natural pyrope appeared to be stable at the two points where it was exposed. Run 29 yielded a mass of well-crystallized dodecahedrons, colorless, isometric with an index of 1.714 ± 0.002; these were embedded in glass. The size ranged up to about 50 micrograms.

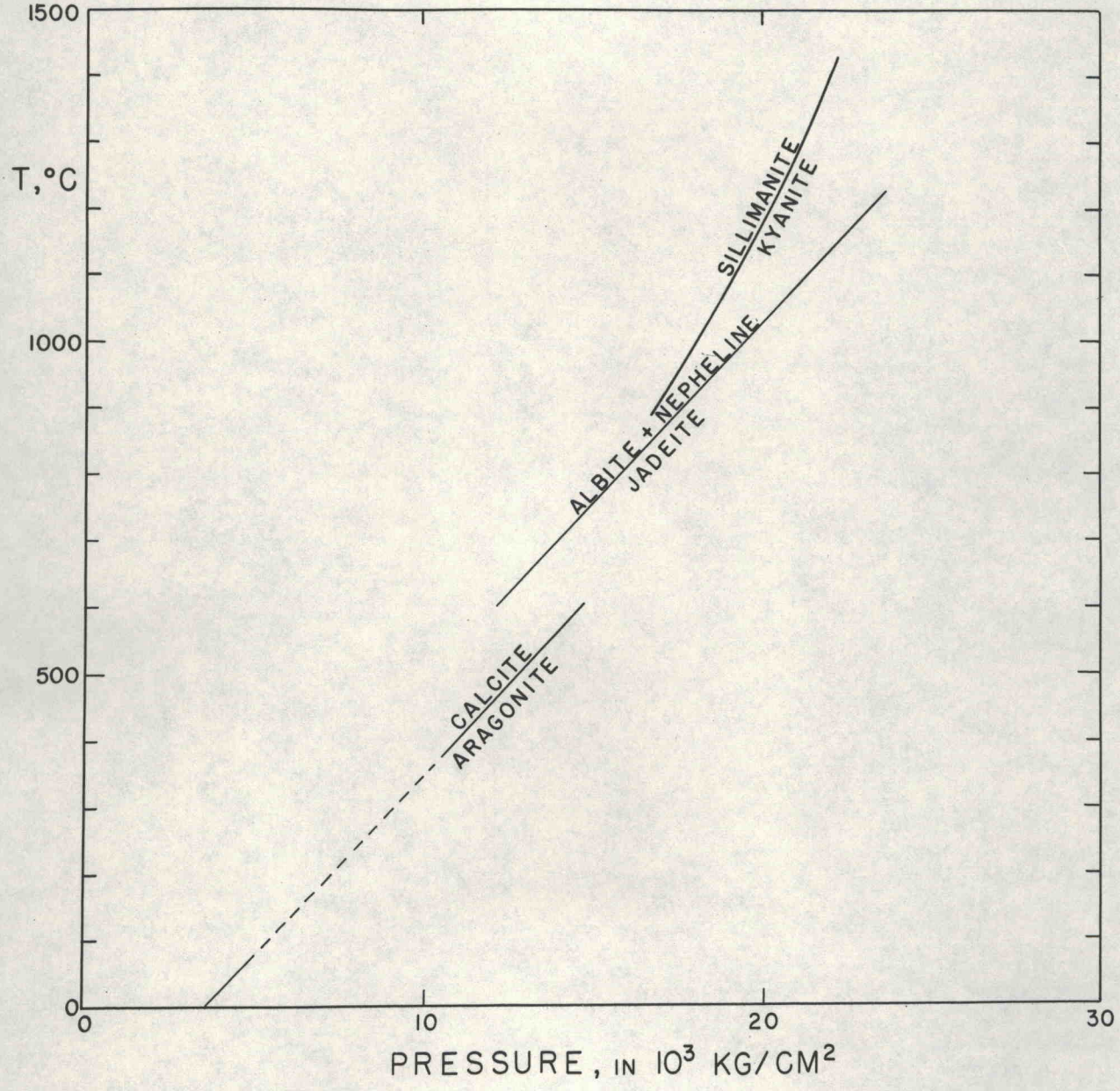

Figure 10. Equilibrium curves determined at high pressures.

Table 7

Crystallization of pyrope

Run	Pressure kg/cm^2	Temperature °C	Duration hours	Charge	Product
29	20,000 ± 500	1020 ± 20	1.0	Pyrope glass plus water	Pyrope
31	21,000 ± 700	900 ± 20	2.0	" "	"
73	25,000 ± 100	1155 ± 20	1.0	" "	"
51	24,900 ± 300	1320 ± 20	1.0	Natural pyrope, dry	"
52	25,900 ± 50	1200 ± 50	1.5	" " plus water	"

Garnets of a wide range of composition have been synthesized by Coes at the Norton Company (Coes, 1955) under comparable conditions of pressure and temperature. For pyrope, the "best condition" are reported to be 30,000 atm. and 900°C, from a mixture of kaolin, silica, magnesia, and magnesium chloride; it is also stated that pyrope "requires a pressure of 30,000 atmospheres at 900°C". The present work indicates that the required pressure at 900°C is closer to 20,000 than to 30,000 atm. for iron - free pyrope, and the equilibrium pressure may be even lower.

Work has also been begun on the reaction, albite $\rightleftharpoons$ jadeite + quartz, for which a theoretical equilibrium curve has been given by Kelly et al (1953; see also Robertson, Birch and MacDonald, 1957). Preliminary results appear to be in good agreement with the thermo-chemical calculations.

High pressure system with solid medium

We have examined (see Appendix) the limitations imposed, first, by the requirement that the elastic limit shall not be exceeded, and second, when plastic deformation is allowed, by the conditions either that residual stresses shall not produce reverse yielding, or the more stringent condition, that the stress difference $/\hat{r}\hat{r}-\hat{z}\hat{z}/$ shall not exceed the stress difference $/\hat{r}\hat{r} - \hat{\theta}\hat{\theta}/$. By the time the greatest allowable internal pressure has been reached, the stresses in the inner cylinder are compressive nearly everywhere, and the system is held together by the tensile stresses in the outer cylinder. The functions of the inner cylinder are then (1) to transmit compressive stress

from the pressure medium to the outer tensile member, (2) to form part of a leak-proof container. It is interesting to follow up the consequences of separating these functions. This may be done in several ways. First, we may imagine a thin continuous liner to contain the pressure fluid, this liner to be supported by the inner cylinder already considered, which may now be segmented or cracked without loss of pressure. Or, second, we may suppose that the pressure medium itself is no longer a fluid but a weak solid, incapable of extrusion through narrow fissures in the container. Once the requirement for continuity of the pressure container is given up, several possibilities arise.

Let us look again at the case of the continuous cylinder already analysed. A sector of such a cylinder is shown in cross-section in Fig. 11. The equilibrium of this sector is maintained by a distribution of normal pressures and tensions, symmetry requiring that there be no shear on the surface indicated. If there are tensile stresses, ("hoop stresses"), then the internal pressure is balanced by the radial component of the tractions on the plane sides of the sector, plus the pressure, if any, on the curved surface, $r = b$. The internal pressure P_a will be greater than wP_b so long as this condition can be maintained; when, however, all of these stresses become compressive, P_a must be less than wP_b; the lateral tractions cannot be made to vanish for a continuous cylinder, but they can be eliminated by dividing the cylinder into a number of sectors with suitable spaces between them.

An approximate solution for an elastic sector with circular boundaries loaded hydrostatically and plane boundaries free from traction is readily obtained. The equations of stress equilibrium are now

$$\frac{\partial \hat{rr}}{\partial r} + \frac{1}{r}\frac{\partial \hat{r\theta}}{\partial \theta} + \frac{\hat{rr} - \hat{\theta\theta}}{r} = 0$$

$$\frac{1}{r}\frac{\partial \hat{\theta\theta}}{\partial \theta} + \frac{\partial \hat{r\theta}}{\partial r} + \frac{2\,\hat{r\theta}}{r} = 0$$

These are satisfied for $\hat{rr} = P_a a/r$, $\hat{\theta\theta} = \hat{r\theta} = 0$; this gives $\hat{rr} = -P_b = -P_a/w$, for $r = b$. But while these stresses satisfy the equations of equilibrium, they do not satisfy the equations of compatibility, and consequently do not constitute a possible solution for a continuous elastic body.

On the other hand, the stresses,
$\hat{rr} = -P\,a\cos\theta / r$, $\hat{\theta\theta} = \hat{r\theta} = 0$,
give the exact solution for a sector loaded symmetrically by a force at the vertex (Timoshenko and Goodier, p. 97). The radial stress is now dependent upon the angle θ, but for sectors of small angle, the approach to a uniform distribution is close. For a 30° sector, the greatest departure from uniformity is only about 3% ($\cos 15^\circ = 0.966$). Thus with sectors of small angle we approach very closely the simple relation, $\hat{rr} = -Pa/r$.

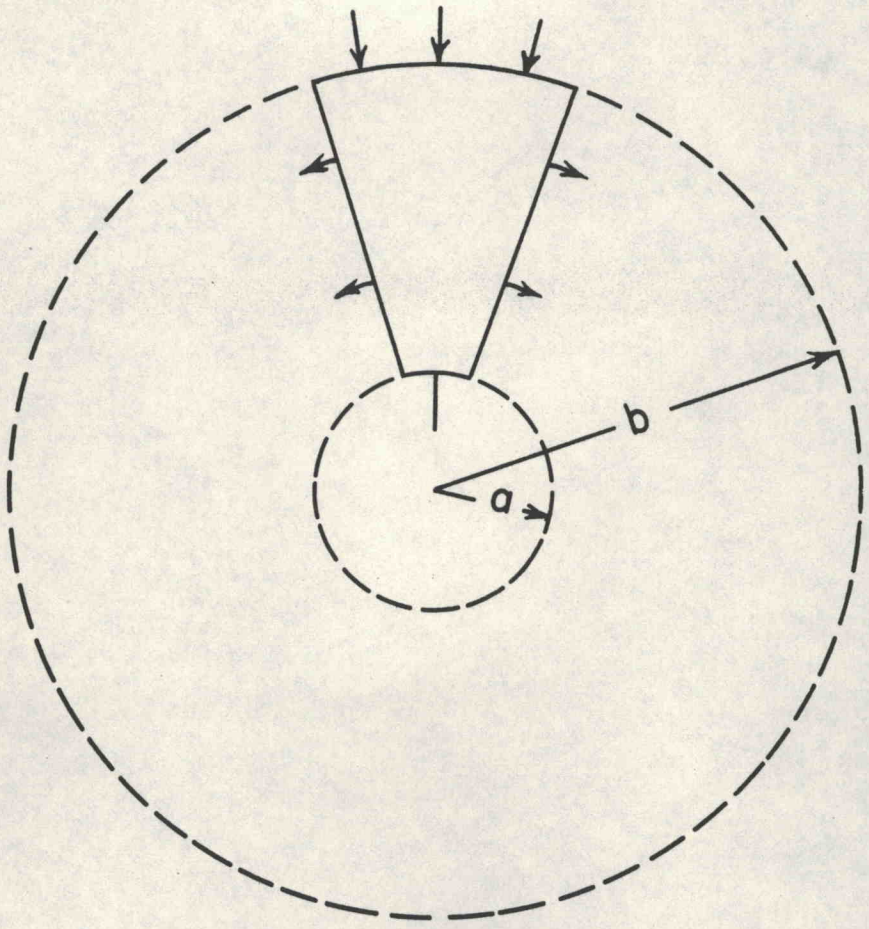

Figure 11. Tractions acting on sector of cylindrical vessel.

The compressive stress is of course greatest at the small end, where it becomes approximately P, and yield or rupture will take place when P equals the strength of the material in simple compression.

With this design it becomes possible to consider the use of very hard materials having high compressive but low tensile strengths. Among these are (1) various steels which can be hardened to give compressive yield points of more than 400,000 psi; (2) cemented carbides, with compressive strengths of perhaps 750,000 psi or more; (3) various refractory non-metals, such as hot-pressed or sintered aluminua, zirconia, etc.; (4) combinations of these. The Norton Company system (for a description and diagram, see the chapter by Roy and Tuttle in Ahrens, Rankama and Runcorn, 1956) employs an inner cylinder of hot-pressed alumina supported by a shrunk-on supporting ring of hardened steel. The wall ratio is about 5 and the system produces its own segmentation in use. Maximum pressures are said to have been 45,000 bars, or about 650,000 psi, the limit being set by the yield of the pistons.

With a "cracked" container of this sort, it is of course convenient to employ a solid pressure medium. The problem of selection of a suitable weak solid then arises, and the choice will depend upon the other properties required, such as electrical and thermal conductivities, chemical stability, compressibility, etc. When the medium is no longer a true fluid, the stress within the medium can, of course, no longer be assumed to be a uniform hydrostatic pressure; it may depart widely from this condition. Any stress may, however, be resolved into a hydrostatic pressure plus shearing stress, and there are a number of materials in which the maximum shearing stresses remain small even at high mean pressures. The investigations of Bridgman on shearing strength under pressure are of especial value here, since many materials show an enormous increase of shearing strength when compressed. Notable for low shearing strength even at high pressure are such soft metals as cadmium, lead, tin, magnesium, indium, zinc, bismuth, calcium, barium, strontium; compounds such as silver chloride, silver sulfate, lead oxide, lead carbonate, and others. Those mentioned have shearing strengths of the order of 2,000 bars at mean pressures of 50,000 bars. Thus the maximum stress difference in such media might be no more than about 4,000 bars, or 8% of a mean pressure of 50,000. There may, of course, be other frictional effects associated with piston motion, so that estimates of pressure based on total force applied to piston area must, unless carefully controlled, be accepted with reserve. Another promising material is limestone (or marble) which has the advantages that (1) it is a fairly good insulator for both heat and electricity, (2) it can be shaped as required to give a starting piece which fills the internal cavity and (3) it has a low initial porosity. The last property is important since it is usually desirable to minimize piston travel in high-pressure systems. The strength

of limestone, especially the Solenhofen lithographic stone, has been investigated by Griggs (1936) and Robertson (1955), with some additional determinations by Robertson in the course of the present work at about 20,000 bars. The stress difference at yielding appears to have an upper limit of about 3,500 ± 500 bars for mean pressures up to 20,000 bars, at ordinary temperature. Higher values were obtained by Bridgman (1937) in his shearing apparatus, with thin layers of the material compressed between hardened steel anvils, thus, at 20,000 bars, the "average shearing stress for steady rotation" was 3500 bars, which corresponds to a stress difference of 7000 bars. No simple explanation of this discrepancy is at hand.

In the various arrangements tried by us, a primary consideration was the combination of high pressures with high temperatures. It is clear that this imposed the need of keeping the tensile parts of the apparatus cool, and consequently of generating the heat internally. This again virtually eliminates the employment of soft metals and turns attention to refractories and insulators. Probably the simplest form of furnace is a graphite or carbon cylinder heated by a large current at low voltage, as in the Norton design. This has been tried, as well as several wire-wound models.

Though none of these systems has as yet been perfected, a number of details may prove interesting to other investigators. One of the simplest arrangements is shown in Figure 12. The pressure chamber is only 1-inch long by 5/8 or 3/4 inch in diameter, and it is supported externally by a heavy ring, into which it is forced by a ram. The moving piston enters on the opposite side. An indication of the frictional effects to be expected is given by some trials in which the medium was AgCl, and the sample a disc, 1/32"- thick, of bismuth. The transition BiI - Bi II and Bi II-Bi III could be detected from the rate of advance of the piston, and the pressures of these transitions have been given by Bridgman. At 27,000 bars, the overall friction was about 10% even with this weak transmitting solid and the short compressed length. Maximum pressures observed, after a correction of 10% for friction, were about 35,000 bars.

Silver chloride begins to conduct electricity appreciably above 300°C, so that it is unsuitable for high-temperature work. Sodium chloride may be used to considerably higher temperatures; and it is about twice as strong as silver chloride at room temperature.

A further development of this kind of system is shown in Figure 13. The cylinder is 2 1/4-inches long, and provided with a porcelain or alumina sleeve, with a bore of 5/8 or 1/2 inch. The medium is limestone, drilled with an axial hole to take a 1/4 inch diameter carbon heater, 1-inch long. The current for this heater passes through the pistons, one of which is insulated from the frameof the press by mica washers. The carbon heater

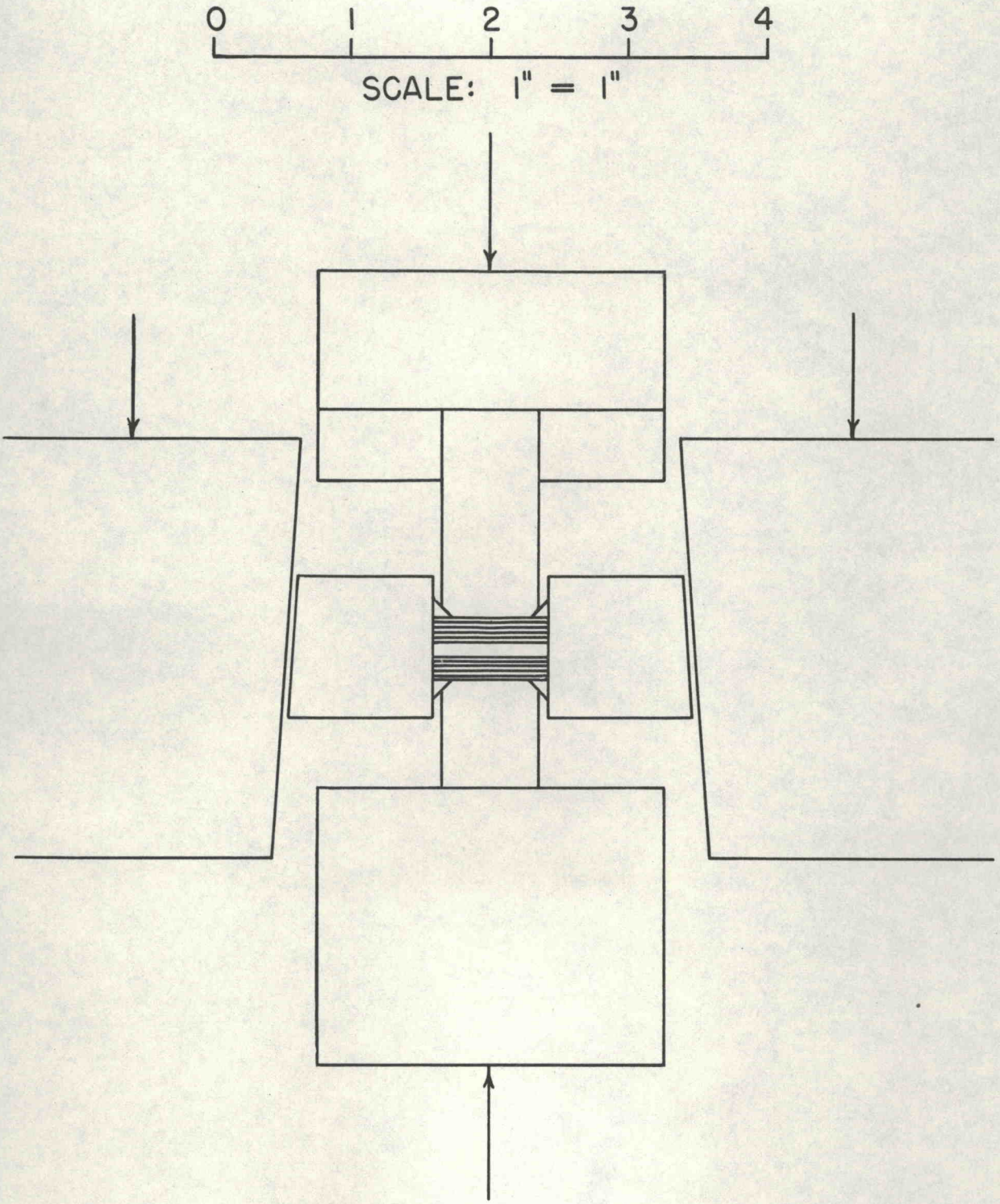

Figure 12. Simple system with solid pressure medium .

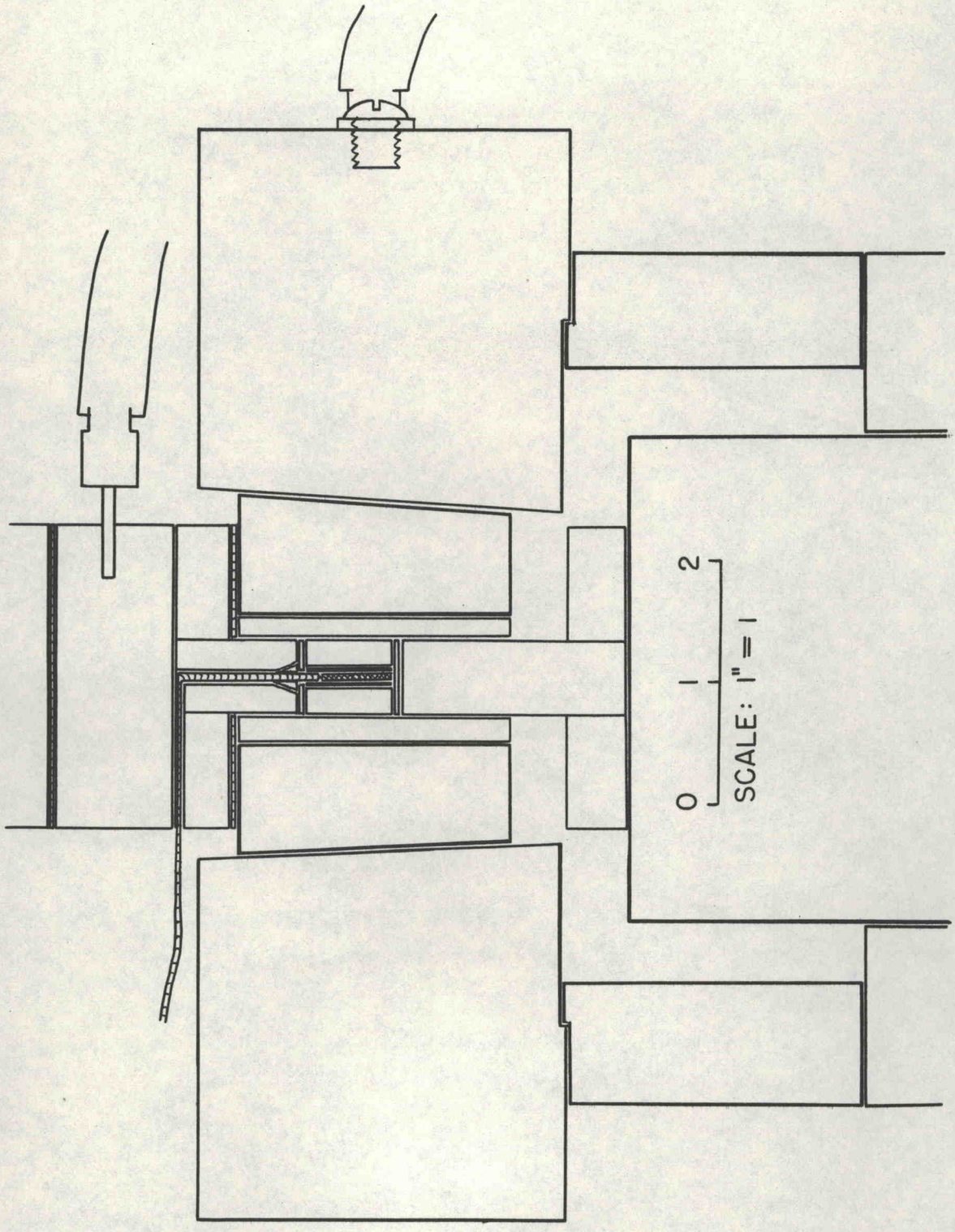

Figure 13. System with solid pressure medium and internal carbon heater.

in turn has an axial hole about 3/16-inch in diameter, in which is placed the sample. This arrangement is much like that of Coes, except that there are no shrink-fitted parts, and the relatively thin porcelain or alumina sleeve replaces the high-density alumina cylinder for electrical insulation while the limestone bushing serves as a plastic pressure medium as well as a thermal insulator. The thin sleeve is broken on each run, but does not come apart until the system is disassembled. No exact data are available as yet on the performance of this arrangement.

Appendix

Introduction

Estimates of various stresses and strains in the compound pressure system are given in the following sections. Though no exact solution has been found for a conical cylinder exposed to different pressures on the internal, uniform bore and on the external, conical surface, we may hope for useful approximations, since the taper is small, based on the known solutions for hollow cylinders of uniform internal and external diameters. We expect that limiting values for the effect of the taper will be given by using, with the solution for a uniform cylinder, the extreme wall ratios at the two ends of the tapered cylinder, since in the actual case the effect of continuity will probably be in the direction of reducing the differences. These differences are not large, the wall ratio remaining between about 3 and 4 for the smaller model, and between 3.3 and 4.7 for the larger one.

Plastic-elastic treatment of inner cylinder

It is helpful to have in mind the solution for a few ideal cases against which to measure the results for the more complex real situations which cannot readily be analyzed. Consider first the infinitely long elastic cylinder with bore radius a, external radius b, internal pressure P_a, external pressure, P_b. Let w be the wall ratio, b/a. The classical solutions for the radial and tangential stresses at radius r are (Love, p.144):

$$\hat{rr} = P_a \frac{(1 - b^2/r^2)}{w^2-1} - P_b \frac{w^2 - b^2/r^2}{w^2-1}$$

$$\hat{\theta\theta} = P_a \frac{1 + b^2/r^2}{w^2 - 1} - P_b \frac{w^2 + b^2/r^2}{w^2 - 1}$$

The stress difference, ignoring for the moment the axial stress, $\hat{zz}$, is

$$\hat{\theta\theta} - \hat{rr} = 2 (P_a - P_b) \frac{b^2/r^2}{w^2 - 1}$$

This is greatest at the bore, r = a, where it is

$$(\hat{\theta\theta} - \hat{rr})_{max} = 2 (P_a - P_b) \frac{w^2}{w^2 - 1}$$

Let us first suppose that yield is determined by the Tresca condition: maximum stress difference equals Y, the yield stress in simple tension. Then we expect yielding for $P_a = P_b + Y (w^2 - 1)/(2w^2)$. For thick-walled cylinders ($w \geq 3$) the pressure at which yield commences is very nearly $P_b + Y/2$.

If the external pressure P_b is produced by another elastic cylinder having no external support, then the upper limit for P_b is $Y'/2$, where Y' is the yield stress of the outer cylinder, and the upper limit for the two-cylinder system in which the stress-difference nowhere exceeds the yield stress is $(Y + Y')/2$. With Y and Y' both of the order of 200,000 psi, the internal pressure cannot exceed about 200,000 psi without producing yield somewhere; the corresponding limit for a single cylinder is 100,000 psi. With the Von Mises condition of yielding, more nearly valid for alloy steels, these values are raised about 15%.

Single cylinders are currently used for pressures up to about 200,000 psi, and have even been pushed to 300,000 psi. These high values are obtained by "overstraining", which has two important effects: first, overstrain increases the yield point by the process known as strain-hardening; second, overstrain produces a redistribution of stress, through yielding near the bore, which is more favorable than the elastic distribution for containing internal pressure. A thick-walled cylinder can be overstrained, or "auto-frettaged" to a point where it can subsequently contain, without further yield, a pressure about twice as great as that required for yielding initially, even without the aid of strain-hardening. Let us suppose that in our two-cylinder system, we can produce $P_b = 200{,}000$ psi. With an elastic inner cylinder, the maximum pressure is $200{,}000 + Y/2$ with the Tresca condition, or perhaps 325,000 psi; this is still appreciably short of the goal of 430,000 psi (30,000 kg/cm^2). In order to obtain the higher figure we must allow plastic deformation of the inner cylinder.

The theory of plastic yielding of a uniform cylinder with a fixed yield point and the Tresca yield condition is given by Hill (1950, p.106 et seq.) The equations are easily generalised to include an external pressure P_b. The cylinder with bore radius a, external radius b, as before, is now taken to be plastic to an intermediate radius c (that is, for $a \leq r \leq c$) and elastic for $c \leq r \leq b$. The solution for the stresses are, for the plastic region:

$$\hat{rr} = Y\left[c^2/2b^2 - 1/2 - \log c/r\right] - P_b$$

$$\hat{\theta\theta} = Y\left[c^2/2b^2 + 1/2 - \log c/r\right] - P_b$$

$$\hat{\theta\theta} - \hat{rr} = Y$$

for the elastic region,

$$\hat{rr} = P_c \frac{c^2(1 - b^2/r^2)}{b^2 - c^2} - P_b \frac{b^2(1 - c^2/r^2)}{b^2 - c^2}$$

$$\hat{\theta\theta} = P_c \frac{c^2(1 + b^2/r^2)}{b^2 - c^2} - P_b \frac{b^2(1 + c^2/r^2)}{b^2 - c^2}$$

with $P_c = P_a - Y \log c/a = P_b + Y(b^2 - c^2)/2b^2$.

The radius c of the plastic-elastic boundary is given by

$$P_a - P_b = Y \left[\log c/a + (1 - c^2/b^2)/2\right] .$$

For the fully plastic condition, $c = b$, and we have $P_a = P_b + \log b/a$ as the maximum internal pressure. If, for example, $b/a = w = 4$, this becomes $P_a = P_b + 1.39\ Y$. With $Y = 250{,}000$ psi and $P_b = 200{,}000$ psi, this gives $P_a = 547{,}000$ psi. For various reasons this is not realizable, but with the same assumptions as to Y and P_b, we reach $P_a = 450{,}000$ psi for $c/a = 1.85$. This is also about the limit consistent with elastic recovery on release of pressure. With the Von Mises condition of yield, this ratio would be reduced to 1.55, which would also suffice to give an internal pressure of 250,000 psi in a single cylinder of $w = 4$, without external support.

An estimate of the residual stresses in an overstrained cylinder may be obtained by adding to the system given above the elastic stresses corresponding to an internal pressure $-P_a$, so that the resultant pressure at the bore will be zero. For a single cylinder with $P_b = 0$, yielding first takes place, on increasing pressure, at, say, $P_o = (Y/2)(1 - a^2/b^2)$. Suppose that the internal pressure is then built up to a higher value P, with propagation of the plastic boundary to radius c. The internal pressure is then released. With the Tresca criterion, the residual strains are then, for $a \leq r \leq c$:

$$\hat{rr} = (Y/2)\left[2 \log r/a - (P/P_o)(1 - a^2/r^2)\right]$$

$$\hat{\theta\theta} = (Y/2)\left[2 \log r/a + 2 - (P/P_o)(1 + a^2/r^2)\right]$$

$$\hat{\theta\theta} - \hat{rr} = Y\left[1 - (Pa^2/P_o r^2)\right] \quad ;$$

for $c \leq r \leq b$,

$$\hat{rr} = -(Y/2)(a^2/r^2 - a^2/b^2)(c^2/a^2 - P/P_o)$$

$$\hat{\theta\theta} = (Y/2)(a^2/r^2 + a^2/b^2)(c^2/a^2 - P/P_o)$$

$$\hat{\theta\theta} - \hat{rr} = Y\,(c^2/a^2 - P/P_o)(a^2/r^2).$$

The residual stress-difference is greatest at the bore, $r = a$, where it is $Y(1 - P/P_o)$. Thus, if the stress-difference is not to exceed Y on release of pressure, after overstrain, P must not exceed $2P_o$ (Hill, p.121). This places a limit on the allowable penetration of the plastic boundary. For $w = 4$, the maximum c/a is about 1.7, and it is not much greater for heavier wall ratios. Thus the very high values of internal pressure corresponding to the fully plastic condition are realizable only at the expense of further yielding in the reverse sense on release of pressure; the equations for residual stresses, moreover, will be valid only for initial overstrains corresponding to $c/a = 1.7$ or less. Since P_o is at most $Y/2$, P will be at most Y for a heavy-walled

autofrettaged cylinder with elastic recovery on release of pressure, on the Tresca condition. With the Von Mises condition, this would be increased to $2Y/\sqrt{3}$, approximately.

The effect of an external pressure P_b which is removed at the same time as the internal pressure P_a, in such a way that no yielding takes place on release, is readily obtained. We need only the stress-difference at the bore; this is found by subtracting the elastic stress-difference, $2w^2(P_a - P_b)/(w^2 - 1)$, from the stress-difference in the plastic zone, Y. If we introduce also the condition at first yielding, $(P_a - P_b)_o = Y(w^2 - 1)/(2w^2)$, then we have a relation, similar to the expression given above for $P_b = 0$, for the residual stress-difference at the bore:

$$(\widehat{\theta\theta} - \widehat{rr})_{res} = Y\left[1 - (P_a - P_b)/(P_a - P_b)_o\right].$$

The condition that this shall not exceed Y is that $(P_a - P_b)$ be less than $2(P_a - P_b)_o$, or less than Y. Thus we must have P_a less or equal to $Y + P_b$. This corresponds to $c/a = 1.8+$ for $w = 4$, 1.65 for infinite w; and the statement made above, that $c/a = 1.85$ corresponds roughly to the limit consistent with elastic recovery, is substantiated.

A special case of some practical interest is that of an external pressure maintained at a given fraction of the internal pressure, say $P_b = xP_a$. For maximum internal pressure consistent with elastic recovery, $P_a = Y/(1 - x)$; if, as in our practice, x is about 1/3, the limiting pressure is 3Y/2, and a yield point of 287,000 psi is required to permit the attainment of an internal pressure of 430,000 psi, on the Tresca condition.

In the foregoing, it has been assumed that the greatest stress-difference is always $\widehat{\theta\theta} - \widehat{rr}$, or in other words, that $\widehat{zz}$ is always intermediate between $\widehat{\theta\theta}$ and $\widehat{rr}$. It is necessary to examine this more closely, since (1) the external pressure may be high enough to transform $\widehat{\theta\theta}$ from tension to compression, and (2) the penetration of the plastic boundary is accompanied by a drop of $\widehat{\theta\theta}$ at the bore and inside the plastic zone. Once $\widehat{\theta\theta}$ has become compressive, or even before if $\widehat{zz}$ were tensile, the possibility arises that the greatest stress-difference may be $\widehat{rr} - \widehat{zz}$, and the problem is drastically altered. In our system, $\widehat{zz}$ is never tensile, but it varies from a fairly high compression at the large end of the tapered cylinder to zero at the small end.

Let us first return to the elastic case. At the bore, $\widehat{\theta\theta} = \left[(w^2+1)P_a - 2w^2 P_b\right] / (w^2 - 1)$. This becomes zero for $P_b/P_a = (w^2 + 1)/(2w^2)$, which equals 17/32 for $w = 4$, and approaches 1/2 for infinite w. With the elastic cylinder, then, $\widehat{\theta\theta}$ becomes compressive only for ratios of P_b/P_a greater than this. If P_b/P_a is maintained at just the ratio necessary to keep $\widehat{\theta\theta} = 0$, then yield begins at $P_a = Y$, regardless of w, if $\widehat{zz}$ is never tensile.

For the plastic-elastic cylinder, $\widehat{\theta\theta} - \widehat{rr} = Y$ in the plastic zone; at the bore, $\widehat{\theta\theta}_a = Y - P_a$, which becomes zero for $P_a = Y$. If $w = 4$, and $P_b/P_a = 1/3$, this pressure is reached for $c/a = 1.25$, about. In order to reach higher pressures, we have to permit greater plastic penetration, and $\widehat{\theta\theta}$ becomes compressive. The distribution of stresses through the wall and the position of the plastic-elastic boundary are illustrated in Fig. 14 for the case just discussed.

For a rough estimate of $\widehat{zz}$, we suppose that the thrust of the lower ram is uniformly distributed over the surface of the conical cylinder, and that the axial stress is uniform over each section normal to the axis, varying from zero at the top of the supporting rings to the maximum value at the bottom. Then we find (see below) $\widehat{zz} = (P_a/3)(w^2 - w_1^2)/(w^2 - 1)$, where w is the wall ratio at any point along the cone, and w_1 the ratio at the top, approximately 3. This varies not quite linearly from zero at the top to $7P_a/45$ at the base. It has been assumed that the thrust of the lower system has been regulated to keep the apparent lateral pressure (see below) equal to $P_a/3$.

As an example, suppose that $c/a = 1.4$; then $\widehat{\theta\theta} = -0.16\ Y$ (compressive), $P_a = 1.16\ Y$; $\widehat{zz}$ runs from 0 to a maximum of $-0.18Y$. Except near the base, $\widehat{\theta\theta}$ is more compressive than $\widehat{zz}$, and the solution based on the assumption that yield begins for a given difference between $\widehat{\theta\theta}$ and $\widehat{rr}$ becomes invalid. We cannot expect, therefore, that the simple solutions based on the Tresca criterion will remain useful much beyond a plastic ratio, $c/a = 1.25$, where the tangential stress becomes zero at the bore. It would be helpful to have corresponding calculations based upon the von Mises criterion of yield, which gives consideration to all three principal stresses. In a qualitative way, however, an explanation has been suggested for the transverse fractures near the small end of the tapered cylinders, because, as the pressure is increased, the point at which $/\widehat{zz} - \widehat{rr}/$ first exceeds $/\widehat{\theta\theta} - \widehat{rr}/$ lies somewhere near the middle of the top supporting ring. The real situation is more unfavorable than this calculation indicates, since the upper ring is the stiffest and hence the lateral pressure is not uniform but is greatest where $\widehat{zz}$ is least.

Elementary theory of conical support.

A simple analysis accounts for the major features of the interaction between tapered cylinder and supporting rings. With reference to Fig. 15, let α be the angle between the axis and generating line of the cone, h the total thickness of the supporting rings, r_1 and r_2 the radii of the openings in the rings at the smaller and larger ends. The cone is pressed into the rings with a total thrust T. Let the normal pressure between rings and cone be N, the coefficient of friction, k. Then the resultant traction on the cone in the direction of the axis is $N(\sin\alpha + k\cos\alpha)$, and in equilibrium we have

$$T = 2\pi \int_{r_1}^{r_2} N\,(1 + k\cot\alpha)\, r\, dr = N\pi(r_2^2 - r_1^2)(1 + k\cot\alpha)$$

if we take N and k to be uniform.

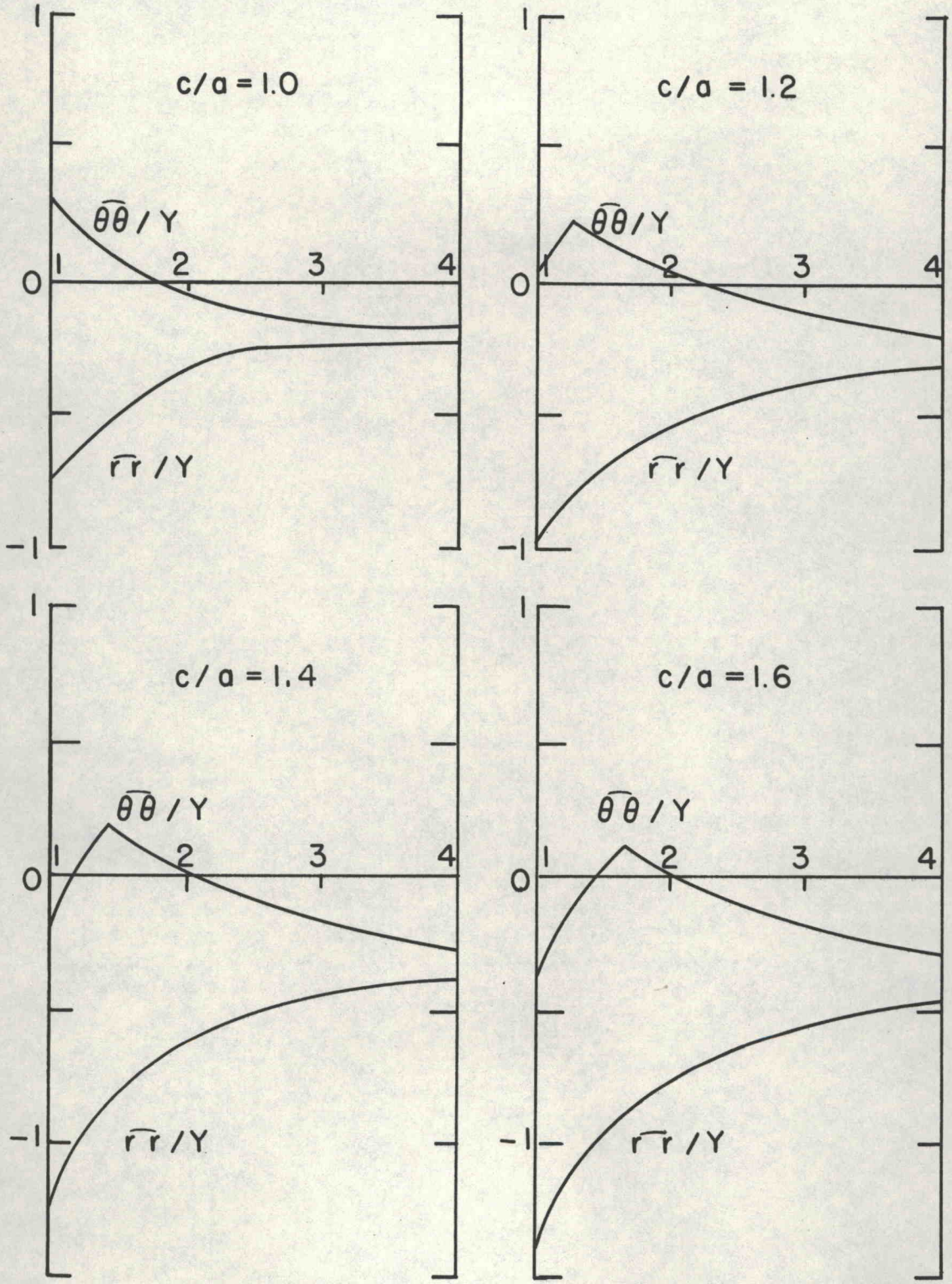

Figure 14. Tangential and radial stresses in the wall of an infinite circular cylinder, with wall ratio = 4, and external pressure equal to one-third the internal pressure. The Tresca condition is satisfied in the plastic zone , $r < c$. Ordinates are stresses divided by Y , abscissae are r/a , where a is the bore radius.

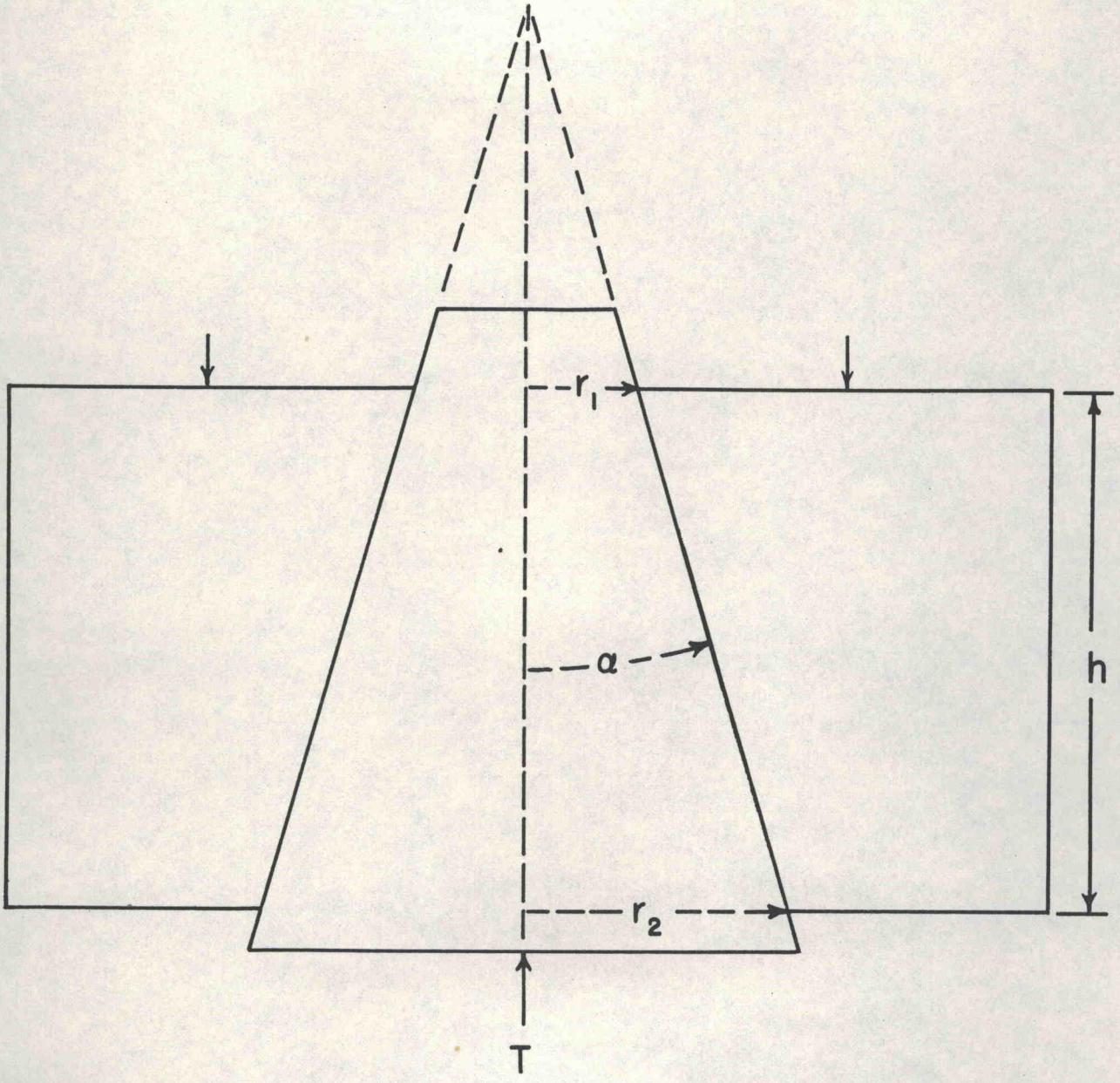

Figure 15. Diagram for discussion of conical support.

Let $No = T / [\pi(r_2^2 - r_1^2)]$, the normal pressure, considered uniform, which would be obtained in the absence of friction. This is what has been called the apparent lateral pressure. With friction, we have $N = No/(1 + 24\,k)$ for our angle, for which $\cot\alpha = 24$. Even a small coefficient of friction produces an appreciable reduction of N, the actual lateral pressure. The experimental curves (Fig. 2, for example) indicate that the friction is not more than about 10% in practice, giving an effective k of about 0.005, a remarkably low figure.

We now examine the assumption that N is uniform. Since the top ring is evidently stiffer than the bottom ring, having a wall ratio of 4 to 4.5 instead of about 3, forcing a cone simultaneously into the two for the same axial distance will produce a greater pressure in the stiffer ring. For a rough estimate of the difference, consider the solution for an infinite cylinder with internal pressure P. Neglecting axial strain, we have for the radial displacement u at the inner surface,

$$u/r = (P/2\mu)\,[w^2 + \mu/(\lambda+\mu)] \;/\; (w^2 - 1)$$

$$= (P/2\mu)\,[(w^2 + 0.43)/(w^2 - 1)]$$

for steel, with $\sigma = 0.285$ and $\lambda/\mu = 1.32$. The value of the coefficient of $P/2\mu$ for several values of w, is as follows:

w	3	4	5
$\frac{w^2+0.43}{w^2-1}$	1.18	1.10	1.06

Consequently, for a given u/r, fixed by the angle of taper, we expect a difference of pressure of only about 10% from one end of the supporting system to the other.

An allowance must be made for the compression of the mandrel or tapered cylinder. For the solid mandrel, the lateral pressure P produces a radial displacement, $u(m)/r = (1 - \sigma)\,P/E$; this is, of course, a contraction. The same pressure P acts to expand the supporting ring, so we have, if u(r) is the displacement of the ring,

$$P = \frac{E\,u(m)/r}{1-\sigma} = 2\mu\,\frac{(w^2 - 1)\,u(r)/r}{w^2 + 0.43}$$

$$\text{whence}\quad u(m)/r = u(r)/r\;\frac{(1-\sigma)(w^2-1)}{(1+\sigma)(w^2+0.43)}$$

The apparent u/r obtained from the advance of the mandrel is the sum of the two terms, since the signs have already been adjusted, and we have

$$u/r\ (\text{apparent}) = u(r)/r\;[1 + 0.556\,(w^2 - 1)/(w^2 + 0.43)]\ .$$

The term added to 1 in the square bracket is approximately 0.5 for w between 3 and 4; hence the actual relative displacement of the ring is about 2/3 of the apparent relative displacement found

by dividing the advance of the mandrel by 12. As an example, consider the figures of ring B (Fig. 2). Advancing the mandrel 0.42 inches into this ring requires a pressure of 9,000 psi on the 5-inch ram. The diameters at the two sides are nearly 2.00 and 2.25 inches. Thus No is 212,000 psi, without allowance for friction. On the other hand, 2u(apparent) is $0.42/12 = 0.035$ inches; 2/3 times this gives 0.023 The mean diameter is 2.125 inches, and thus u(r)/r is 0.011. From this we obtain for the pressure, 237,000 psi; 2μ has been taken as $23.3 \cdot 10^6$ psi, and the mean w as 9/2.125 or 4.24. The agreement is probably as good as can be expected for so rough a calculation.

When the hollow inner cylinder is forced into the rings, the stiffest supporting ring engages the least stiff part of the inner cylinder. For an external pressure P upon a uniform cylinder, the hoop stress $\theta\theta$ at the bore is $\theta\theta = -2w^2P/(w^2 - 1)$, where w is now the wall ratio for the inner cylinder. The factor $w^2/(w^2-1)$ varies from 1.125 for $w = 3$ to 1.065 for $w = 4$. Taking into account the circumstance that when $w = 3$ for the inner cylinder, it is approximately 4 for the outer ring, with a reversal of these values toward the other end, we find that $\theta\theta$ will vary from a quantity proportional to 1.02 at the upper end, to 0.90 at the lower, or 13% in all. This does not yet allow for the greater relative contraction of the hollow cylinder at the upper end, which tends to reduce this difference.

In order to estimate this, we calculate the displacement u at the outer surface of a uniform, infinite, cylinder subjected to external pressure P; if we put $e_{zz} = 0$, then

$$u/r = -(P/2\mu)\ \frac{1 + \mu w^2/(\lambda+\mu)}{w^2 - 1} = -\frac{P\,(1+\sigma)}{E}\ \frac{(0.43w^2 + 1)}{(w^2 - 1)}$$

The factor of P/E is shown below as function of w:

w	2	3	4	5	∞
$(1+\sigma)\frac{0.43w^2 + 1}{w^2 - 1}$	1.17	0.78	0.68	0.63	0.553

The values for $w = 3$ and $w = 4$ differ by about 15% and in the direction to cancel out (and slightly reverse) the difference in $\theta\theta$ obtained above without this allowance.

We notice also that the factor given here for $w = \infty$ (the solid mandrel) differs from the factor 0.715 given above. This is because in the former calculation we took the axial stress, zz, to be zero, whereas we now are supposing the axial strain e_{zz} to be zero. For the solid mandrel, if we put $e_{zz} = 0$, we find $u/r = (P/E)(1 - \sigma - 2\sigma^2) = 0.553P/E$, in agreement with the result for the hollow cylinder of infinite wall ratio. Neither of these assumptions about the axial stress or strain is strictly correct, and we cannot expect to obtain highly accurate values for strains and displacements, even apart from the approximations involved in neglecting the taper.

We have also to take into account the effect of the internal pressure P_a in the inner cylinder. This expands the inner cylinder and hence increases the effective interference with the supporting rings. Because of the taper, this will not be uniform over the conical surface. An estimate may be obtained of the stress $\hat{rr}$ at various radii corresponding to those of the outer surface of the tapered cylinder in a single elastic cylinder having the overall dimensions of tapered cylinder and supporting rings combined. We have $\hat{rr} = P_a\,(1 - g^2/r^2)/(w^2 - 1)$, where we now take $w = 12$, $g = 4.5$ inches. For ready comparison with the results for uniform external pressure P_b and for the ratio, $P_b = P_a/3$, the results are expressed as $\hat{rr}/P_b$:

2r, inches	2	2.25	2.5	2.75	3	3.25
$-\hat{rr}/P_b$	0.477	0.372	0.297	0.240	0.198	0.165

Thus the difference between the extreme upper end ($2r = 2$ inches) and the bottom ($2r = 2.75$ inches) from this cause might be as much as 24% of P_b; the difference between the point at the bottom of the upper ring ($2r = 2.25$ inches) and the bottom might amount to 13% of P_b.

The distribution of $\hat{zz}$ along the inner cylinder is a matter of some interest in connection with the failure of this component. At any point, at which the outer radius is r, we have, as a mean value,

$$\hat{zz} = T(r)/\cdot[\pi(r^2 - a^2)],$$

a being the radius of the bore, i.e. 0.375 inches.

Now $$T(r) = 2\pi\int_{r_1}^{r} N(1 + k\cot\alpha)\, r\, dr$$

and hence for uniform N,

$$\hat{zz} = N_o\,(r^2 - r_1^2)\,/\,(r^2 - a^2) = N_o\,(w^2 - w_1^2)\,/(w^2 - 1).$$

The notation is as above, N_o being the uncorrected pressure obtained by dividing the thrust T by the area of the conical surface projected on a plane normal to the axis. The distribution of mean $\hat{zz}$ is thus as follows:

z, inches	= 0	2.25	4.5	6.75	9
w	= 3 (= w_1)	3.35	3.5	3.75	4
$\hat{zz}/N_o$	= 0	0.167	0.289	0.389	0.467

As we have seen N, or P_b, is not quite uniform, but may be some 35% or so greater at the small end than at the large end of the tapered cylinder. This would mean a somewhat more rapid increase of $\hat{zz}$ on passing from the small end toward the large end than is indicated by these figures.

Effect of discontinuities of load:

It is interesting to look for weaknesses associated with the discontinuities of internal and external loading. The

principal effect is located in the neighborhood of the piston packing; on one side, there is the pressure P_a; in the soft packing, this rises to about 1.2 P_a and then falls abruptly to zero. This change takes place in an axial distance of the order of 1/16 inch, and it is clear that there must be localized shearing stress of considerable magnitude. This can be calculated, at least so long as it remains within the elastic range, with the aid of curves and tables prepared at the Watertown Arsenal Laboratory and compiled in the "Thickwalled Tube Handbook" by Radkowski, Bluhm and Bowie. These calculations are for internal and external normal and shear loading applied to tubes of infinite length over the interval $-\infty < z < 0$; the discontinuity is at $z = 0$. The z-axis is the axis of symmetry. Though strictly valid only for tubes of infinite length, the calculations show a rapid diminution of the effects of the discontinuous loadings with axial distance from the discontinuity; a few bore diameters away from this point, the effects are usually negligible, and no important errors result from direct application of these calculations to our situation.

Consider first the discontinuity of internal pressure; the Handbook furnishes values of the stresses $\hat{\theta\theta}$ and $\hat{zz}$ at the bore, as function of distance from the discontinuity, for $w = 2.5$, which is close enough to the actual value for purposes of illustration. These are plotted in Figure 16. The greatest stress difference is always $\hat{\theta\theta}-\hat{rr}$; $\hat{zz}$ is in fact compressive on the pressure side of the discontinuity.

In the neighborhood of the discontinuity, $\hat{rr}$ and $\hat{zz}$ are no longer principal stresses; a shear $\hat{rz}$ appears, which reaches an appreciable fraction of P close to the discontinuity, at a small depth below the internal surface. The maximum value appears to be about 0.3 P, and it is very sharply localized. The total shear energy, however, is still smaller than in the portions of the bore remote from the packing. The stress gradients are, of course, extremely high near the discontinuity, even in the real, smoothed-out, case, and there have been suggestions that these may influence failure (Hill, p. 124).

Another effect of the discontinuity is produced by the friction in the packing. The total friction may amount to some 10% of the total force on the piston, occasionally more. Thus there is a band of shear at the packing, having an average value, per unit area, of $0.1 \frac{a}{2t} P$ or $0.3P$ for $t = 1/16"$. Now the calculations for a semi-infinite discontinuous shear loading lead to infinities for $\hat{\theta\theta}$ and $\hat{zz}$ at the discontinuity; with a discontinuous band, there will be two infinities, a compressive one for the leading edge, and a tensile one for the following edge. The infinities arise from the assumption that the band of shear begins and ends with sharp corners, and this is not possible in the real situation; nevertheless, very high values may be produced locally, both of $\hat{\theta\theta}$ and $\hat{zz}$. The effect of the bank of shear is to exaggerate, by a considerable but unknown amount, the local

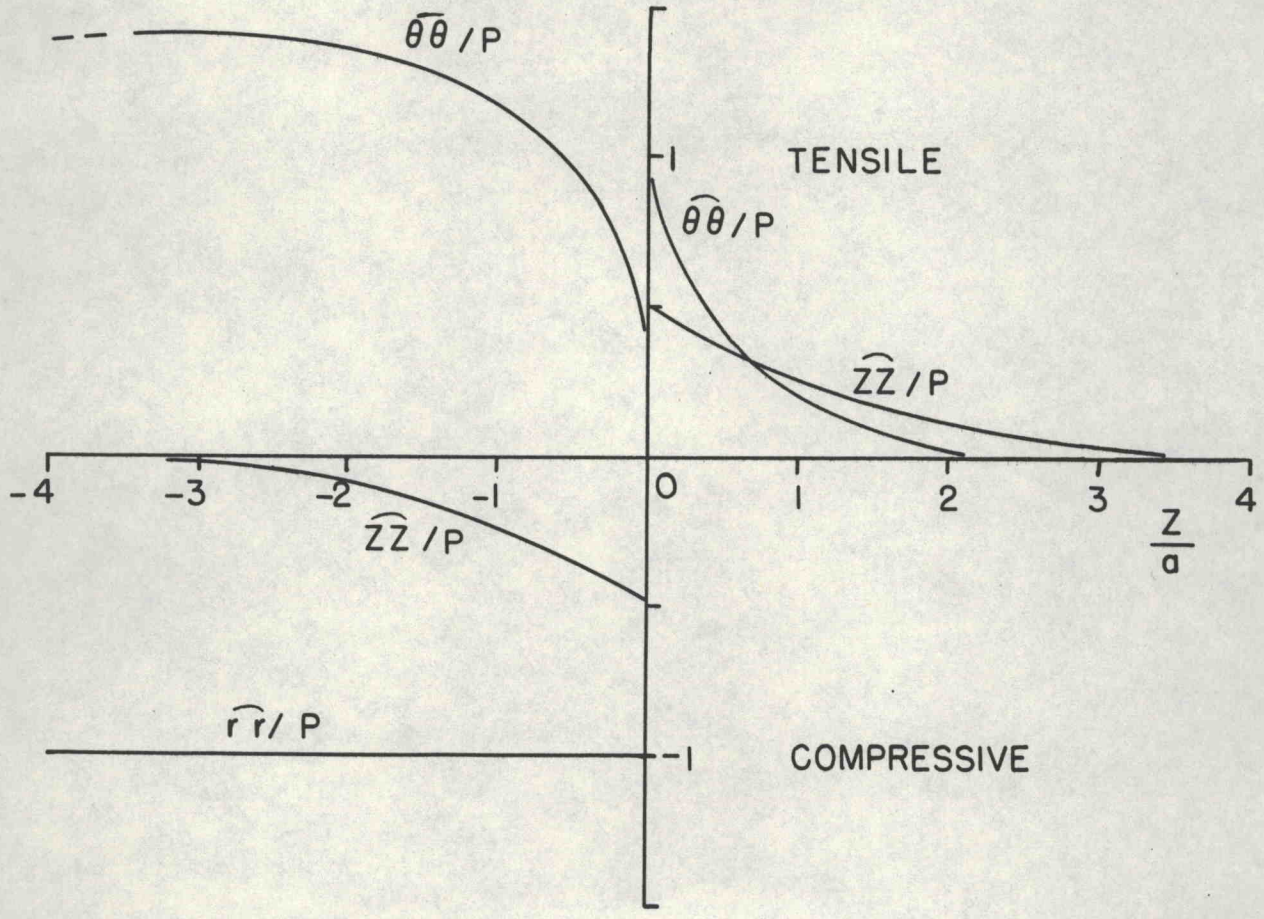

Figure 16. Stresses associated with a discontinuity of internal pressure P in an infinite cylinder of wall ratio 2.5 , after Radkowski, Bluhm and Bowie. The pressure acts on the bore, of radius a, at all points to the left of the origin ($z < 0$) ; it is zero for $z > 0$. The ordinates are stresses divided by P ; the abscissae are z/a.

discontinuities of both $\theta\theta$ and zz. Reduction of packing friction to a minimum is evidently important. Several instances of rupture beginning at the packing have been observed.

The external tractions produced by the supporting rings are also discontinuous, and estimates of the stresses, in the elastic case, produced at the bore of the inner cylinder may be based on the calculations for external pressure and shear loadings given in the "Handbook". Because of the thickness of the inner cylinder, the effects of the external discontinuities are much smoothed out at the bore, and rough calculations show that these effects are unlikely to be of consequence.

REFERENCES

1. Ahrens, L. H., Rankama, K. and Runcorn, S. K., 1956: Physics and Chemistry of the Earth, Vol. 1, 317 pages, McGraw-Hill, New York; Pergamon Press, London.

2. Benedict, Manson, 1937: Pressure, volume, temperature properties of nitrogen at high density. I. Results obtained with a weight piezometer. II. Results obtained by a piston displacement method., J. Am Chem. Soc. 59, p. 2224 and 2233.

3. Birch, Francis, 1939: Thermoelectric measurement of high temperatures in pressure apparatus, Rev. Sci. Instr. 10, p. 137/140.

4. Bridgman, P.W., 1931: The Physics of High pressure, G. Bell and Son, London, 398 pages: Rev. Ed. 1952, 445 pages.

5. _____, 1935a, Measurements of certain electrical resistances, compressibilities and thermal expansions to 20,000 kg/cm^2, Proc. Amer. Acad. Arts and Sci. 70, p. 71-101.

6. _____, 1935b, The melting curves and compressibilities of nitrogen and argon, ibid. 70, p. 1-32.

7. _____, 1937, Shearing phenomena at high pressures, particularly in inorganic compounds, ibid. 71, p. 387-460.

8. _____, 1937, Polymorphic Transitions of 35 substances to 50,000 kg/cm^2, ibid. 72, p. 45-136.

9. _____, 1938, Resistance of 19 metals to 30,000 kg/cm^2, ibid. 72, p. 157-205.

10. _____, 1940, The measurement of hydrostatic pressure to 30,000 kg/cm^2, ibid. 74, p. 1-10.

11. Clark, S. P., Jr., 1954: A note on calcite-aragonite equilibrium Amer. Mineralogist, in press.

12. Clark, Sidney P., Jr., Robertson, Eugene C., and Birch, Francis, 1957: Experimental determination of kyanite - sillimanite equilibrium relations at high temperatures and pressures, Am. J. Sci., in press.

13. Coes, L., Jr., 1953: A new dense crystalline silica, Science, 118, p. 131-132.

14. Coes, L., Jr. 1953: High-pressure minerals, J. Amer. Ceramic Soc. 38, p. 298.

15. Domb, C., 1951: The melting curve at high pressures, Phil. Mag. 42, 1316-1324.

16. Griggs, D. T. and Kennedy, G. C., 1956: A simple apparatus for high pressure and temperatures, Am. J. Sci. 254, p. 722-735.

17. Griggs, D. T., 1936: Deformation of rocks under high confining pressures, J. Geol. 44, p. 544-571.

18. Hill, R., 1950, The Mathematical Theory of Plasticity, Oxford, Clarendon Press: 354 pages.

19. Jamieson, J. C., 1953: Phase equilibrium in the system calcite-aragonite, J. Chem. Phys. 21, p. 1385-1390.

20. Kelley, K.U., Todd, S.S., Orr, R.L., King, E.G., and Bonnickson, K.R., 1953: Thermodynamic properties of sodium-aluminum and potassium-aluminum silicates, U. S. Bur. of Mines, Report of inv. 4955.

21. Love, A. E. H., 1927: A treatise on the mathematical theory of elasticity, 4th ed., 643 pages, Cambridge Univ. Press.

22. MacDonald, Gordon J. F., 1956: Experimental determination of calcite-aragonite equilibrium relations at elevated temperatures and pressures, Amer. Mineral. 41, p. 744-756.

23. Mills, R. L. and Grilly, E. R., 1955: Melting curves of He^3, He^4, H_2, D_2, Ne, N_2, and O_2 up to 3500 kg/cm , Phys. Rev. 99, p. 480-486.

24. Radkowski, P. P., Bluhm, J. I., Bowie, O. L., 1954, Thick-walled Cylinder Handbook, Watertown Arsenal, WAL No. 893/172, 171 pages.

25. Robertson, E. C., 1955: An experimental study of the strength of rocks, Bull. Geol. Soc. Amer., 66, p. 1275-1314.

26. Robertson, Eugene C., Birch, Francis and MacDonald, Gordon J.F., 1957: Experimental determination of jadeite stability relation to 25,000 bars, Am. J. Sci. 225, p. 115-137.

27. Robinson, D. W., 1954: An experimental determination of the melting curves of argon and nitrogen into the 10,000 atm. region, Proc. Roy. Soc. A225, p. 393-405.

28. Salter, L., 1954: The Simon melting equation, Phil. Mag. 45, p. 369-378.

29. Simon, F. E., 1937: Range of Stability of the fluid state, Trans. Faraday Soc. 33, p. 65-73.

30. Simon, F. E., Ruhemann, M. and Edwards, W. A. M., 1930: Die Schmelzkurven von Wasserstoff, Neon, Stickstoff und Argon, Z. Phys. Chem. B,6, p. 331.

31. Timoshenko, S., and Goodier, J. N., 1951: Theory of Elasticity, McGraw-Hill, N. Y., 506 pages.

DISTRIBUTION LIST

Technical, Summary and Final Reports

Contract N5ori, 07644 — Task No. NR-032400

Chief of Naval Research
Department of the Navy
Washington 25, D. C.
Attn: Code 423 (2)
: Code 421 (1)

Director,
Office of Naval Research
Branch Office
495 Summer Street
Boston, Massachusetts

Assistant Naval Attache for Research
Office of Naval Research
Branch Office
Navy 100
Fleet Post Office
New York, New York (5)

Director,
Naval Research Laboratory
Washington 25, D. C.
Attn: Technical Information Officer (6)

Director,
Office of Technical Services
Department of Commerce
Washington 25, D. C.

Armed Services Technical Information Agency
Documents Service Center
Knott Building
Dayton 2, Ohio (5)

Director,
Naval Research Laboratory
Washington 25, D. C.
Attn: Code 6300, Metallurgy Div.
: Code 2020, Technical Library

Bureau of Aeronautics
Department of the Navy
Washington 25, D. C.
Attn: N. E. Promisel, AE41
: Technical Library, TD41

Commanding Officer
Naval Air Materiel Center
Naval Base Station
Philadelphia, Pennsylvania
Attn: Aeronautical Materials Lab.

Bureau of Ordnance
Department of the Navy
Washington 25, D. C.
Attn: Re
: Technical Library, Ad3

Superintendent, Naval Gun Factory
Washington 25, D. C.
Attn: Metallurgical Lab., DE 713

Commanding Officer,
U. S. Naval Ordnance Laboratory
White Oaks, Maryland

Commanding Officer,
U. S. Naval Ordnance Test Station
Inyokern, California

Bureau of Ships
Department of the Navy
Washington 25, D. C.
Attn: Code 343
: Code 337L, Tech. Library

U. S. Naval Engineering Experiment Station
Annapolis, Maryland
Attn: Metals Laboratory

Director, Materials Laboratory
Building 291
New York Naval Shipyard
Brooklyn 1, New York
Attn: Code 907

Bureau of Yards and Docks
Department of the Navy
Washington 25, D. C.

Post Graduate School
U. S. Naval Academy
Monterey, California

Office of the Chief of Ordnance
Research and Development Service
Department of the Army
Washington 25, D. C.
Attn: ORDTB

Commanding Officer
Office of Ordnance Research
Duke University
Durham, North Carolina
Attn: Metallurgy Division

Commanding Officer
Watertown Arsenal
Watertown, Massachusetts
Attn: Laboratory Division

Director,
Ordnance Materials Research Office
Watertown Arsenal
Watertown, Massachusetts

Commanding Officer
Frankford Arsenal
Frankford, Pennsylvania
Attn: Laboratory Division

Office of the Chief of Engineers
Department of the Army
Washington 25, D. C.
Attn: Research and Development Branch

Air Research and Development Command
Office of Scientific Research
Washington, D. C.
Attn: Solid State Sciences Division

Wright Air Development Center
Wright-Patterson Air Force Base
Dayton, Ohio
Attn: Materials Laboratory
: Aeronautical Research Lab.(MCRR)

Atomic Energy Commission
Division of Research
Metallurgy and Materials Branch
Washington 25, D. C.

National Bureau of Standards
Washington 25, D. C.
Attn: Metallurgy Division (2)
: Mineral Products Division (2)

National Advisory Committee
for Aeronautics
1512 H Street, N. W.
Washington 25, D. C.

Lewis Flight Propulsion Laboratory
National Advisory Committee for
Aeronautics
Cleveland, Ohio

Argonne National Laboratory
P. O. Box 299
Lemont, Illinois

Brookhaven National Laboratory
Technical Information Division
Upton, New York
Attn: Research Library

Carbide & Carbon Chemicals Division
Plant Records Department
Central Files (K-25)
P. O. Box P
Oak Ridge, Tennessee

General Electric Company
Technical Services Division
Technical Information Group
P. O. Box 100
Richland, Washington
Attn: Miss M. G. Freidank

Iowa State College
P. O. Box 14A, Station A
Ames, Iowa
Attn: Dr. F. H. Spedding

Knolls Atomic Power Laboratory
P. O. Box 1072
Schenectady, New York
Attn: Document Librarian

Los Alamos Scientific Laboratory
P. O. Box 1663
Los Alamos, New Mexico
Attn: Reports Librarian

Oak Ridge National Laboratory
P. O. Box P
Oak Ridge, Tennessee
Attn: Central Files

Sandia Corporation
Sandia Base
Classified Document Division
Albuquerque, New Mexico

U. S. Atomic Energy Commission
Technical Information Service
P. O. Box 62
Oak Ridge, Tennessee

University of California
Radiation Laboratory
Information Division
Room 128, Building 50
Berkeley, California
Attn: Dr. R. K. Wakerling

Westinghouse Electric Corporation
Atomic Power Division
P. O. Box 1468
Pittsburgh 30, Pennsylvania
Attn: Librarian

New York State College of Ceramics
Alfred University
Alfred, N. Y.
Attn: Dr. J. F. McMahon,
Dean

University of Utah
Salt Lake City, Utah
Attn: Dr. Henry Eyring
Attn: Dr. S. S. Kistler

University of Michigan
Mineralogical Laboratory
Ann Arbor, Mich.
Attn: Dr. C. B. Slawson

Pennsylvania State University
University Park, Pa.
Attn: Dr. W. A. Weyl

University of California
Division of Mineral Technology
Berkeley, Calif.
Attn: Dr. J. A. Pask
Attn: Dr. A. W. Searcy

North Carolina State College
Department of Engineering Research
Raleigh, N. C.
Attn: Mr. N. W. Conner

Polytechnic Institute of Brooklyn
99 Livingston Street
Brooklyn, N. Y.
Attn: Dr. Benjamin Post

U. S. Bureau of Mines
Pacific Experiment Station
126 Hearst Memorial Mining Building
Berkeley, Calif.
Attn: Dr. K. K. Kelley

New Jersey Ceramic Research Station
Rutgers, the State University
New Brunswick, N. J.
Attn: Dr. John H. Koenig